

The Effect of Pressure Pulsations and Vibrations on Fully Developed Pipe Flow

Donald O. Barnett
ARO, Inc.

August 1981

Final Report for Period October 1977 – September 1978

Approved for public release; distribution unlimited.

ARNOLD ENGINEERING DEVELOPMENT CENTER
ARNOLD AIR FORCE STATION, TENNESSEE
AIR FORCE SYSTEMS COMMAND
UNITED STATES AIR FORCE

NOTICES

When U. S. Government drawings, specifications, or other data are used for any purpose other than a definitely related Government procurement operation, the Government thereby incurs no responsibility nor any obligation whatsoever, and the fact that the Government may have formulated, furnished, or in any way supplied the said drawings, specifications, or other data, is not to be regarded by implication or otherwise, or in any manner licensing the holder or any other person or corporation, or conveying any rights or permission to manufacture, use, or sell any patented invention that may in any way be related thereto.

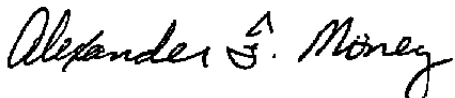
Qualified users may obtain copies of this report from the Defense Technical Information Center.

References to named commercial products in this report are not to be considered in any sense as an indorsement of the product by the United States Air Force or the Government.

This report has been reviewed by the Office of Public Affairs (PA) and is releasable to the National Technical Information Service (NTIS). At NTIS, it will be available to the general public, including foreign nations.

APPROVAL STATEMENT

This report has been reviewed and approved.



ALEXANDER F. MONEY
Aeronautical Systems Division
Deputy for Operations

Approved for publication:

FOR THE COMMANDER



MARION L. LASTER
Director of Technology
Deputy for Operations

UNCLASSIFIED

UNCLASSIFIED

UNCLASSIFIED

20. ABSTRACT, Concluded.

equations can be solved and the axial momentum equation is linearized so that the velocity field can be obtained as the sum of a steady and a time-dependent component. By obtaining a solution for the case where the pressure (or amplitude of vibration) varies sinusoidally, one obtains the solution for disturbances of arbitrary waveform through a Fourier series expansion of the disturbance. Results are presented that show that the velocity field is dependent upon the mean flow Reynolds number, a vibrational Reynolds number, and the amplitude of the forcing function. In general, the fluid response to differing waveforms is similar to that obtained for simple harmonic oscillations with respect to the various parameters explored. The temporal history at a given location, however, may differ radically since over much of the tube diameter the velocity is a simple integral transform of the forcing function.

PREFACE

The work reported herein was conducted by the Arnold Engineering Development Center (AEDC), Air Force Systems Command (AFSC). The initial work was performed by ARO, Inc. (a Sverdrup Corporation Company), operating contractor for the AEDC, AFSC, Arnold Air Force Station, Tennessee, under ARO Project Number E32A-POA. The report was written under the direction of Dr. C. E. Peters, ARO, Inc., and the manuscript was submitted for publication on July 14, 1980.

The author gratefully acknowledges the contribution of Mr. E. W. Dorrell, Jr., ARO, Inc., who programmed and ran the two computer codes developed in the course of the study.

Dr. D. O. Barnett is currently a member of the faculty of the School of Engineering at the University of Alabama in Birmingham.

CONTENTS

	<u>Page</u>
1.0 INTRODUCTION	5
2.0 FLUID RESPONSE TO LONGITUDINAL PULSATIONS	6
2.1 Formulation in Noninertial Frame	7
2.2 Dimensional Analysis	10
2.3 Specification of the Pressure Field	12
2.4 Simple Harmonic Pulsations	15
2.5 Pulsations of Arbitrary Waveform	22
3.0 THE VELOCITY FIELD FOR SIMPLE HARMONIC PULSATIONS	25
3.1 Theoretical Results	25
3.2 Comparisons with Experiment	35
4.0 THE VELOCITY FIELD FOR ARBITRARY WAVEFORMS	38
4.1 Effect of Waveform	38
4.2 Fluid Response to a Fluttering Valve	46
5.0 CONCLUSIONS AND RECOMMENDATIONS	48
REFERENCES	51

ILLUSTRATIONS

Figure

1. Comparison of Inertial and Tube-Fixed Coordinate Systems	6
2. Variation of Velocity Profile Parameters with Reynolds Number	18
3. Comparison of Theoretical and Experimental Velocity Distributions in Steady Turbulent Flow	19
4. Velocity and Eddy Viscosity Distributions in Steady, Fully Developed Flow in a Tube	19
5. Temporal Variation of Local Velocity for Harmonic Forcing Function	26
6. Phase Lag of the Velocity for a Simple Harmonic Pulsation	27
7. Temporal Variation of Velocity for Several Reynolds Numbers	28
8. Influence of Vibrational Reynolds Number on Transient Velocity Component	31
9. Temporal and Amplitude Dependence of Transient Centerline Velocity	32
10. Effect of Vibrational Reynolds Number on RMS Velocity Component	33

<u>Figure</u>	<u>Page</u>
11. Variation of Transient Component Maximum Value Location with Frequency	34
12. Near-Wall Velocity Profiles for Turbulent Exchange Modification	35
13. Comparison of Experiment and Theory in Laminar Pulsating Flow	36
14. Comparison of Experiment and Theory in Turbulent Pulsating Flow	37
15. Symmetric Forcing Functions	39
16. Centerline Velocity Response to Symmetric Waves	41
17. Convergence of Transient Velocity Series for Square Wave Excitation	42
18. Comparison of Velocity Response to Square Wave at Several Radial Locations	44
19. Velocity Distribution for Various Times During a Cycle	45
20. Effect of Frequency on Amplitude and Radial Distribution of Transient Velocity Component	46
21. Asymmetric Wave Forms	47
22. Centerline Velocity Response to Asymmetric Waves	48
23. Distribution of Transient Velocity with Radial Location	49
 APPENDIXES	
A. Formulation for Arbitrary Eddy Viscosity Model	53
B. A Note on Complex Fourier Expansions	56
 NOMENCLATURE	58

1.0 INTRODUCTION

Many naturally occurring flows as well as those encountered in engineering applications are time dependent. In such cases the velocity field responds to an imposed pressure gradient or other external excitation in an extremely complex fashion. To illustrate the possible effects of time-varying conditions on fluid response, it is useful to consider a class of internal flows that are called (equivalently) pulsating, pulsatile, or oscillating. Such flows are characterized by temporally periodic variations of the imposed pressure, which may result from (1) unstable combustion processes, (2) acoustic disturbances, (3) vibrations at flow boundaries, (4) the action of reciprocating pumps, or (5) unstable pressure regulators and valves. It is known from analysis (Refs. 1 through 4) and has been demonstrated experimentally (Refs. 5 through 8) that flow pulsations may (1) promote transition to turbulence, (2) alter the turbulent structure of the flow, (3) cause flow reversals during a portion of a cycle, and (4) significantly augment or, in some cases, inhibit heat transfer. The velocity field, moreover, varies in its response to a periodic pressure disturbance with the peak velocity amplitude lagging the peak pressure amplitude by as much as 90 deg (i.e., one-fourth the period of the disturbance) on the centerline of a tube. Perhaps the most striking feature of bounded, pulsating flows is the observation that the maximum fluid velocity frequently does not occur on the centerline of the duct or pipe so that (1) a greater portion of the mass flow is carried in the annular region near the wall and (2) the instantaneous wall shear stress may be significantly greater than in steady flows at the same Reynolds number.

It is obvious that, even in this relatively simple case, transient fluid motions may introduce effects that cannot be ignored in conducting, or analyzing data from, experimental studies. The complexity of the phenomena is such, moreover, that attempting to draw conclusions on the basis of quasi-steady models is not advisable and often is a serious error. In view of these considerations, it is necessary to develop practical computational models that will allow the determination of the details of a variety of transient flows common in AEDC test facilities to serve as a guide for both the establishment of test procedures and the interpretation of test data.

Undoubtedly, the most general way to obtain reliable models of transient fluid phenomena will be through the development of finite difference or finite element models which solve the governing partial differential equations. Pending the development of such programs and as an aid in their evaluation it is useful to develop mathematically exact solutions to those specific problems which lend themselves to exact analysis. Various analytical solutions have been proposed for the velocity field on pulsating flows. Sexl (Ref. 9) obtained a solution for the velocity field in a tube in which only a purely oscillatory flow

existed. His results were extended by Uchida (Ref. 2) to pulsatile flow superimposed on a laminar mean fluid motion. Although Uchida's formulation is valid for pulsations of arbitrary waveform, his results consider only the case of simple harmonic oscillations. Romie (Ref. 3) treated the velocity and temperature field in laminar pipe flows subjected to simple harmonic pressure pulsations in a study of heat-transfer mechanisms. The velocity field in the developing flow near the entrance of a tube was treated by Atabek and Chang (Ref. 10). Barnett (Ref. 4) obtained the velocity and temperature fields in turbulent pulsating flows in determining the effect of simple harmonic longitudinal vibrations on heat transfer in a tube.

It is the purpose of this study to obtain a solution for the velocity field in a fully developed, turbulent pipe flow subjected to excitation by longitudinal disturbances of arbitrary waveform. The particular cases to be studied will include (1) simple harmonic pulsations (sinusoidal variation in time) of the pressure field or longitudinal vibrations of the tube, (2) coupled pressure pulsations and vibrations, and (3) pressure pulsations of arbitrary waveform.

2.0 FLUID RESPONSE TO LONGITUDINAL PULSATIONS

The subject of this study is the motion of a fluid in a pipe when the fluid experiences pulsations induced either by a time-varying pressure field or by longitudinal vibrations of the tube. Two candidate cylindrical reference frames for formulating the problem are shown in Fig. 1. In the inertial reference frame (r' , θ' , z), the "no-slip" condition at the tube wall ($r = R$) requires specification of a nonhomogeneous, time-dependent velocity at the boundary when the tube is vibrating. If, on the other hand, a similarly oriented coordinate system (r , θ , z) is chosen to move at the velocity of the wall, a homogeneous boundary

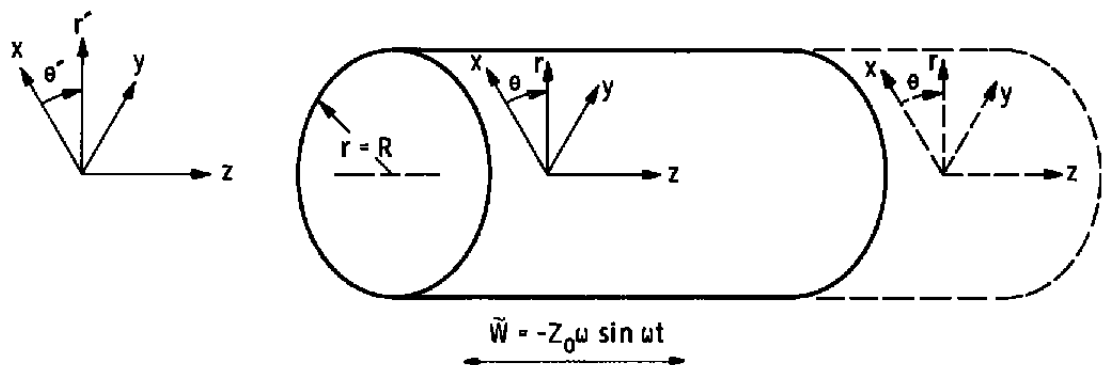


Figure 1. Comparison of inertial and tube-fixed coordinate systems.

condition will result, and the problem is simpler from a mathematical viewpoint. This latter system, however, is noninertial, and the momentum equations must be modified to account for this fact.

2.1 FORMULATION IN NONINERTIAL FRAME

The continuity, momentum, and energy equations for the isothermal flow of an isotropic, Newtonian fluid in a noninertial coordinate system (Ref. 4) are given below.

Continuity:

$$\frac{D\rho}{Dt} + \rho\Delta = 0 \quad (1)$$

Momentum:

$$\rho \frac{D\mathbf{v}}{Dt} = \rho \mathbf{X}_i - \frac{\partial \mathbf{p}}{\partial \mathbf{x}_i} - \rho \frac{d\tilde{\mathbf{v}}_i}{dt} - \frac{2}{3} \frac{\partial}{\partial \mathbf{x}_i} \left[(\mu - \mu_b) \Delta \right] - \frac{\partial}{\partial \mathbf{x}_j} \left[\mu \left(\frac{\partial v_i}{\partial \mathbf{x}_j} + \frac{\partial v_j}{\partial \mathbf{x}_i} \right) \right] \quad (2)$$

Energy:

$$\frac{p}{\rho} \frac{D\rho}{Dt} + \mu\Phi = 0 \quad (3)$$

where

$$\frac{D}{Dt} = \frac{\partial}{\partial t} + \mathbf{v}_j \frac{\partial}{\partial \mathbf{x}_j} \quad , \quad \Delta = \frac{\partial \mathbf{v}_i}{\partial \mathbf{x}_j} \quad , \quad \text{and} \quad \Phi = \text{dissipation function.}$$

Comparing these equations to those obtained for an inertial coordinate system, one sees that they differ only by the term $\rho(d\tilde{\mathbf{v}}_i/dt)$, which appears in the momentum equation. The vector $\tilde{\mathbf{v}}_i$ is the velocity of the moving reference relative to a fixed frame. For a simple harmonic oscillation of frequency, ω , and amplitude, Z_0 , directed along the Z-axis,* the following relations may be established between the coordinate systems of Fig. 1:

$$r' = r \quad , \quad \theta' = \theta \quad , \quad z = z + Z_0 \cos \omega t \quad (4)$$

*Note that more complex vibrations may be treated by introducing the appropriate reference motion here.

Thus, if \tilde{U} , \tilde{V} , \tilde{W} are the components of the coordinate system velocity vector, \tilde{V}_i , then

$$\tilde{U} = \tilde{V} = 0 \quad \text{and} \quad \tilde{W} = -Z_0 \omega \cos \omega t \quad (5)$$

The relations (1) through (3) and (5) are adequate to describe the laminar flow of fluid in a longitudinally vibrating tube. To obtain a formulation suitable for turbulent flows as well, it is convenient to decompose any dynamic variable, B (such as pressure and velocity), into the sum of a statistical mean value, $\bar{B} = b$, and a fluctuating component, $b'(t)$. Thus:

$$\begin{aligned} V_i &= v_i + v'_i & | \\ P &= p - p' & | \end{aligned} \quad (6)$$

It should be noted that if temporal averages are utilized, the period, T , over which the average

$$b = \frac{1}{T} \int_0^T B(t) dt$$

is obtained must be small with respect to the period of the imposed oscillation to allow the mean value to be time dependent. Introducing Eqs. (4) and (6) into Eqs. (1) through (3), assuming the fluid to be incompressible, and taking the average of the resulting equations in accordance with Reynolds rules (Ref. 11) leads to the following relations with respect to the noninertial cylindrical reference system:

Continuity:

$$\frac{1}{r} \frac{\partial}{\partial r} (ru) + \frac{1}{r} \frac{\partial v}{\partial \theta} - \frac{\partial w}{\partial z} = 0 \quad (7)$$

r-Momentum

$$\begin{aligned} \frac{\partial u}{\partial t} + u \frac{\partial u}{\partial r} + \frac{v}{r} \frac{\partial u}{\partial \theta} - \frac{v^2}{r} - w \frac{\partial u}{\partial z} &= -\frac{1}{\rho} \frac{\partial p}{\partial r} \\ + \nu \left[\frac{1}{r} \frac{\partial}{\partial r} \left(r \frac{\partial u}{\partial r} \right) - \frac{u}{r^2} + \frac{1}{r^2} \frac{\partial^2 u}{\partial \theta^2} - \frac{2}{r^2} \frac{\partial v}{\partial \theta} + \frac{\partial^2 u}{\partial z^2} \right] \\ - \left[\frac{\partial}{\partial r} (\bar{u}'^2) - \frac{1}{r} \frac{\partial}{\partial \theta} (\bar{u}' \bar{v}') + \frac{\partial}{\partial z} (\bar{u}' \bar{w}') + \frac{\bar{u}'^2 - \bar{v}'^2}{r} \right] \end{aligned} \quad (8)$$

θ -Momentum:

$$\begin{aligned}
 \frac{\partial v}{\partial t} + u \frac{\partial v}{\partial r} + \frac{v}{r} \frac{\partial v}{\partial \theta} + \frac{w}{r} \frac{\partial v}{\partial z} &= -\frac{1}{\rho r} \frac{\partial p}{\partial \theta} \\
 &+ \nu \left[\frac{1}{r} \frac{\partial}{\partial r} \left(r \frac{\partial v}{\partial r} \right) - \frac{v}{r^2} + \frac{1}{r^2} \frac{\partial^2 v}{\partial \theta^2} + \frac{2}{r^2} \frac{\partial v}{\partial \theta} + \frac{\partial^2 v}{\partial z^2} \right] \\
 &- \left[\frac{\partial}{\partial r} (\bar{u}' \bar{v}') + \frac{1}{r} \frac{\partial}{\partial \theta} (\bar{v}'^2) + \frac{\partial}{\partial z} (\bar{v}' \bar{w}') + \frac{2}{r} (\bar{u}' \bar{v}') \right] \quad (9)
 \end{aligned}$$

 z -Momentum:

$$\begin{aligned}
 \frac{\partial w}{\partial t} + u \frac{\partial w}{\partial r} + \frac{v}{r} \frac{\partial w}{\partial \theta} + w \frac{\partial w}{\partial z} &= -\frac{1}{\rho} \frac{\partial p}{\partial z} + Z_o \omega^2 \cos \omega t \\
 &- \nu \left[\frac{1}{r} \frac{\partial}{\partial r} \left(r \frac{\partial w}{\partial r} \right) - \frac{1}{r^2} \frac{\partial^2 w}{\partial \theta^2} + \frac{\partial^2 w}{\partial z^2} \right] \\
 &- \left[\frac{\partial}{\partial r} (\bar{u}' \bar{w}') + \frac{1}{r} \frac{\partial}{\partial \theta} (\bar{v}' \bar{w}') + \frac{\partial}{\partial z} (\bar{w}'^2) + \frac{\bar{u}' \bar{w}'}{r} \right] \quad (10)
 \end{aligned}$$

The energy equation, Eq. (3), simply states that the dissipation, Φ , is zero.

These equations may be greatly simplified under the following assumptions: (1) the mean flow is rectilinear, so that $u = v = 0$; (2) the mean velocity field is axisymmetric; and (3) all correlations $(\bar{v}_i \bar{v}_j)$ are axisymmetric and invariant in the axial direction. The first and third assumptions restrict the analysis that follows to the hydrodynamically fully developed region of a tube. For steady, turbulent flows the condition is usually obtained within 10 tube diameters from the entrance of the tube for $Re \geq 10,000$ (Ref. 12).

For these assumptions, the continuity equation reduces to the statement that $w = w(r, t)$. The momentum equations reduce to:

 r -Momentum:

$$\frac{1}{\rho} \frac{\partial p}{\partial r} - \frac{\partial}{\partial r} (\bar{u}'^2) + \frac{\bar{u}'^2 - \bar{v}'^2}{r} = 0 \quad (11)$$

 θ -Momentum:

$$\frac{\partial}{\partial r} (\bar{u}' \bar{v}') + \frac{2}{r} (\bar{u}' \bar{v}') = 0 \quad (12)$$

z-Momentum:

$$\frac{\partial w}{\partial t} = -\frac{1}{\rho} \frac{\partial p}{\partial z} + Z_0 \omega^2 \cos \omega t - \frac{\nu}{r} \frac{\partial}{\partial r} \left(r \frac{\partial w}{\partial r} \right) - \frac{1}{r} \frac{\partial}{\partial r} (r \overline{u' w'}) \quad (13)$$

The formulation of the problem is completed upon specification of the boundary conditions. For a no-slip condition at the tube wall it is required that

$$w(R, t) = 0 \quad (14)$$

Several other restrictions must also be imposed: (1) any solution must be symmetric about $r = 0$; (2) any solution must be finite; and (3) all transient effects must vanish as the amplitude or frequency of pulsation becomes zero. Since flow near the tube boundary is known to be laminar, all correlations must vanish at the wall. No initial condition will be imposed upon the problem. Any solution to be obtained will, therefore, be quasi-steady and correspond to conditions existing after the initial transients have been damped.

2.2 DIMENSIONAL ANALYSIS

It is convenient and instructive to obtain a dimensionless system of equations equivalent to those obtained above. To this end the following dimensionless independent variables are introduced:

$$\tau = \omega t \quad ; \quad \eta = \frac{r}{R} \quad ; \quad \zeta = \frac{z}{R} \quad (15)$$

The dependent variables are taken to be

$$\Omega(\eta, \zeta, \tau) = \frac{p - p^*}{\rho U^*^2} \quad ; \quad V(\eta, \tau) = \frac{w}{U^*} \quad (16)$$

where the friction velocity is

$$U^* = \sqrt{\frac{\langle \sigma_w \rangle}{\rho}} \quad (17)$$

(Angle brackets, $\langle \rangle$, denote the average over a cycle of the pulsation.) The reference pressure, p^* , is taken to be the pressure at the entrance to the tube. The correlations are defined by

$$R_{v_i v_j} = \frac{\langle v'_i v'_j \rangle}{U^*^2} \quad (18)$$

Substitution of Eqs. (15) through (18) into Eqs. (11) through (13) leads to the following:

η -Momentum:

$$\frac{\partial \Omega}{\partial \eta} - \frac{\partial R_{uu}}{\partial \eta} + \frac{R_{uu} - R_{vv}}{\eta} = 0 \quad (19)$$

θ -Momentum:

$$\frac{\partial R_{uv}}{\partial \eta} + 2 \frac{R_{uv}}{\eta} = 0 \quad (20)$$

ξ -Momentum:

$$Re_v \frac{\partial V}{\partial \tau} = -Re^* \frac{\partial \Omega}{\partial \zeta} + \frac{A Re_v^2}{Re^*} \cos \tau + \frac{1}{\eta} \frac{\partial}{\partial \eta} \left(\eta \frac{\partial V}{\partial \eta} \right) - \frac{Re^*}{\eta} \frac{\partial}{\partial \eta} (\eta R_{uw}) \quad (21)$$

where

$$Re_v = \frac{\omega R^2}{\nu} \quad (22)$$

is the dimensionless frequency or vibrational Reynolds number,

$$Re^* = \frac{U^* R}{\nu} \quad (23)$$

is the friction Reynolds number, and

$$A = \frac{Z_o}{R} \quad (24)$$

is the dimensionless amplitude.

The amplitude of a pressure pulse will be determined later (see Section 2.3), but is of the form

$$A_p = \frac{\Omega_1(1, \infty)}{\Omega_n(1, \infty)} \quad (25)$$

where $\Omega_1(1, \infty)$ is the amplitude of the time-dependent component of the wall pressure coefficient far from the entrance of the tube and $\Omega_0(1, \infty)$ is the amplitude of the steady flow component.

In view of these equations, it is clear that the velocity field in a fully developed, pulsating flow is given by a relation of the form

$$V = V(\eta, \tau, \text{Re}^*, \text{Re}_v, A, A_p) \quad (26)$$

The friction Reynolds number is related to the conventional Reynolds number, $\text{Re} = 2\langle \tilde{U} \rangle R/\nu$, where \tilde{U} is the spatially averaged velocity in the tube, by

$$\text{Re}^* = \text{Re} \sqrt{\frac{C_f}{8}}$$

where C_f is the Fanning friction factor (Ref. 12). When the mean velocity $\langle \tilde{U} \rangle = 0$, the friction Reynolds number vanishes and must be replaced in the ζ -momentum equation by the harmonic Reynolds number (Ref. 7):

$$\text{Re}_h = \frac{\omega R Z_o}{\nu} = A \text{Re}_v$$

The velocity, pressure coefficient, and correlations for no mean through flow are thus nondimensionalized with respect to the harmonic velocity, $U_h = \omega Z_o$.

2.3 SPECIFICATION OF THE PRESSURE FIELD

Consideration must first be given to determining the form of the pressure coefficient for various types of pulsations. Although an exact formulation will not be obtained, the functional behavior of the pressure field will provide sufficient information to allow a solution of the momentum equations.

The θ -momentum equation, Eq. (20), may be integrated immediately to obtain

$$R_{uv} = \frac{C}{\eta^2} \quad (27)$$

For the correlation to vanish at the tube wall ($\eta = 1$), it follows that $C = 0$ and $R_{uv} = 0$ everywhere in the tube.

Direct integration of the n -momentum equation, Eq. (19), is also possible, and one obtains

$$\Omega(\eta, \zeta, \tau) = \Omega(1, \zeta, \tau) + F_{\Omega}(\eta, \tau) \quad (28)$$

where

$$-F(\eta, \tau) = R_{uu}(\eta, \tau) \cdot \int_1^{\eta} \frac{R_{uu} - R_{uv}}{\eta} d\eta$$

Note that while the pressure varies across the tube in a turbulent flow, this variation is independent of the axial coordinate provided the flow is fully developed. For this case, moreover, it is reasonable to assume that at any given axial station the wall pressure coefficient will exhibit a temporal behavior similar to the excitation applied at the entrance to the tube. Consequently, for a simple harmonic pressure oscillation,

$$\Omega(1, \zeta, \tau) = C_1 \zeta \left[\Omega_0(1, \infty) - \Omega_1(1, \infty) \cos \tau \right] + C_2(\tau) \quad (29)$$

where $\Omega_1(1, \infty)$ is the mean value over a cycle of the wall pressure coefficient in the fully developed region and $\Omega_1(1, \infty)$ is the amplitude of the variation about the mean. At $\zeta = 0$, it follows that

$$C_2(\tau) = \Omega(1, 0, \tau) = \Omega_0(1, 0) + \Omega_1(1, 0) \cos \tau \quad (30)$$

if the waveform is undistorted. From Eqs. (29) and (30) it follows that

$$\Omega(1, \zeta, \tau) = C_1 \zeta \Omega_0(1, \infty) (1 + A_p \cos \tau) + \Omega_0(1, 0) (1 + A_{p_0} \cos \tau) \quad (31)$$

From Eqs. (28) and (31), the ζ -momentum equation becomes

$$\begin{aligned} Re_v \frac{\partial v}{\partial r} = -C_2 Re^* \Omega_0(1, \infty) (1 + A_p \cos \tau) + \frac{A_p Re_v^2}{Re^*} \cos \tau \\ + \frac{1}{\eta} \frac{\partial}{\partial \eta} \left(\eta \frac{\partial v}{\partial \eta} \right) - Re^* \frac{1}{\eta} \frac{\partial}{\partial \eta} (\eta R_{uw}) \end{aligned} \quad (32)$$

Now the dimensionless mass flow through the tube is

$$G^* = \frac{\dot{m}}{\rho U^* R^2} = 2\pi \int_0^1 \langle V \rangle \eta d\eta \quad (33)$$

If this value is to remain constant over a cycle of the pulsation, it follows that $\partial \langle V \rangle / \partial \tau = 0$. Accordingly, averaging Eq. (32) over a cycle leads to

$$Re^* C_2 \Omega_o (1, \infty) = \frac{1}{\eta} \frac{\partial}{\partial \eta} \left(\eta \frac{\partial \langle V \rangle}{\partial \eta} \right) - Re^* \frac{1}{\eta} \frac{\partial}{\partial \eta} (\eta \langle R_{uw} \rangle) \quad (34)$$

Multiplying Eq. (34) by η and integrating gives

$$\eta \frac{\partial \langle V \rangle}{\partial \eta} - Re^* \eta \langle R_{uw} \rangle = Re^* C_2 \Omega_o \frac{\eta^2}{2} + C_4 \quad (35)$$

Evaluating Eq. (35) on the centerline of the tube shows that $C_4 = 0$. Furthermore, at the wall $\langle R_{uw} \rangle = 0$; thus

$$C_2 = \frac{2}{Re^* \Omega_o (1, \infty)} \left. \frac{\partial \langle V \rangle}{\partial \eta} \right|_{\eta=1} \quad (36)$$

From Newton's law of viscosity it follows directly that

$$\left. \frac{\partial \langle V \rangle}{\partial \eta} \right|_{\eta=1} = -Re^*$$

So that

$$C_2 = -\frac{2}{\Omega_o (1, \infty)} \quad (37)$$

The pressure coefficient variation in the fully developed region is, thus,

$$\Omega(\eta, \zeta, \tau) = -2\zeta(1 + A_p \cos \tau) + \Omega_o(1, 0)(1 + A_{p_o} \cos \tau) \quad (38)$$

From Eq. (38), the ξ -momentum equation becomes

$$Re_v \frac{\partial V}{\partial \tau} = \mathcal{F}(\tau) + \frac{1}{\eta} \frac{\partial}{\partial \eta} \left(\eta \frac{\partial V}{\partial \eta} \right) - \frac{Re^*}{\eta} \frac{\partial}{\partial \eta} (\eta R_{uw}) \quad (39)$$

where, for simple harmonic pulsations, the forcing function, $\mathcal{F}(\tau)$, is

$$\mathcal{F}(\tau) = 2 Re^* (1 + \mathcal{G} \cos \tau) \quad (40)$$

with a generalized amplitude defined by

$$\mathcal{G} = A_p - \frac{A Re_v^2}{2 Re^{*2}} \quad (41)$$

It is noted, moreover, that while Eq. (39) was obtained for the case where pressure pulsations and vibrations of a common frequency were the forcing function for the transient fluid motion, the case of tube vibration alone ($A_p = 0$) or pressure pulsations alone ($A = 0$) are also obtained. In fact, any pulsation for which $\partial \Omega / \partial \xi = \mathcal{F}(\tau)$ can be treated by simply expanding $\mathcal{F}(\tau)$ in a complex Fourier series, as will be shown in Section 2.5.

2.4 SIMPLE HARMONIC PULSATIONS

It has been shown that for simple harmonic vibrations of a tube and/or pressure pulsations, the velocity field in axisymmetric, fully developed flow of a constant property fluid must satisfy a differential equation of the form of Eq. (39). Since this relation is linear, a solution is sought which will consist of a periodic motion superimposed on the mean flow. Thus, let

$$V(\eta, \tau) = V_o(\eta) + V_1(\eta, \tau) \quad (42)$$

Similarly, in analogy with the Boussinesq exchange hypothesis (Ref. 11),

$$R_{uw} = -\frac{1}{\nu Re^*} \left[\epsilon_{n_o}(\eta) \frac{dV_o}{d\eta} + \epsilon_{m_1}(\eta) \frac{\partial V_1}{\partial \eta} \right] \quad (43)$$

Substitution of Eqs. (41) through (43) into Eq. (39) allows one to separate the ξ -momentum equation into

$$\frac{1}{\eta} \frac{d}{d\eta} \left[\left(1 + \frac{\epsilon_{m_o}}{\nu} \right) \eta \frac{dV_o}{d\eta} \right] + 2 Re^+ = 0 \quad (44)$$

for the mean velocity component, and

$$Re^+ \frac{\partial V_I}{\partial \tau} = G \cos \tau + \frac{1}{\eta} \frac{\partial}{\partial \eta} \left[\left(1 + \frac{\epsilon_{m_I}}{\nu} \right) \eta \frac{\partial V_I}{\partial \eta} \right] \quad (45)$$

for the transient component of velocity. The boundary conditions corresponding to Eq. (14) are $V_o(1) = 0$ and $V_I(1, \tau) = 0$.

2.4.1 The Mean Velocity Component

Equation (44) and its boundary conditions are identical to the Reynolds equation and boundary conditions for fully developed, "steady" turbulent flow in a tube. Since turbulent flow solutions rely on agreement with experimental data as well as with the governing equations, many semi-empirical solutions to that problem have been proposed. Due to its inherent simplicity, the solution proposed by Pai (Ref. 13) will be used.

The velocity variation across the tube is given by

$$V_o(\eta) = V_c \left(1 + \frac{s-m}{m-1} \eta^2 + \frac{1-s}{m-1} \eta^{2m} \right) \quad (46)$$

where $V_c = V_o(0)$. This relation is an exact solution of the Reynolds equation if the eddy diffusivity is

$$1 + \frac{\epsilon_{m_o}}{\nu} = \left[\frac{m-s}{s(m-1)} + \frac{m(s-1)}{s(m-1)} \eta^{2m-2} \right]^{-1} \quad (47)$$

The empirical coefficients must be chosen so that the velocity profile accurately represents the experimental data.

If one differentiates Eq. (46) and evaluates the result at $\eta = 1$, it follows that

$$s = \frac{Re^*}{2V_c} \quad (48)$$

The parameters "s" may be interpreted as the ratio of the wall shear stress in a turbulent flow to that in a laminar flow with the same centerline velocity (Ref. 13). For $s = 1$, Eq. (46) reduces to the fully developed laminar flow profile, and the eddy diffusivity vanishes. To evaluate "m" it is only necessary to require that the mean velocity predicted by the profile should match those velocities experimentally observed. Thus (Ref. 4),

$$m = \frac{s - 2 \frac{\hat{V}}{V_c}}{2 \frac{\hat{V}}{V_c} - 1} \quad (49)$$

From these relations, it is readily shown that for any specified mean velocity, \hat{V} , both empirical constants can be determined if the wall shear stress, $\langle \sigma_w \rangle$, and the centerline velocity, V_c , are known. Figure 2, based on the data of Haberstroh and Baldwin (Ref. 14), presents the values of the empirical constants for $4,000 \leq Re \leq 200,000$. For Reynolds numbers in excess of 10,000, both parameters are accurately described by the power law relations shown in the figure.

Figure 3 compares Pai's relation (Eq. 46) to data obtained by Nikuradse for $Re = 23,000$. The agreement is good over the entire tube radius although Pai's result underpredicts the experimental data by about 10 percent near the wall. Figure 4 shows the velocity profile and eddy diffusivity variation across the tube for several Reynolds numbers. It is noted that for high Reynolds numbers ϵ_{m_0}/ν approaches a constant value across the tube. This observation will be of some importance in the following section.

2.4.2 The Transient Velocity Component

Noting that $\cos \tau = \operatorname{Re}(e^{i\tau})$ suggests a solution to Eq. (45) of the form

$$V_I(\eta) = \operatorname{Re} \left[f(\eta) e^{i\tau} \right] \quad (50)$$

Making this substitution in Eq. (45), one obtains

$$\left(1 + \frac{\epsilon_{m1}}{\nu} \right) f'' + \frac{1}{\eta} \left[1 + \frac{\epsilon_{m1}}{\nu} + \frac{\eta \epsilon'_{m1}}{\nu} \right] f''' - i \operatorname{Re} \sqrt{f} = -\bar{Q} \quad (51)$$

where primes denote differentiation with respect to η . The boundary condition corresponding to a no-slip requirement at the wall is simple $f(1) = 0$.

Equation (51) can be solved by numerical techniques for any arbitrary eddy viscosity distribution. One procedure for obtaining such a solution is presented in Appendix A. The main objection to such solutions, however, is a lack of definitive experimental data on the nature of the turbulent exchange process in pulsating flows. Bogdonoff (Ref. 6) concluded

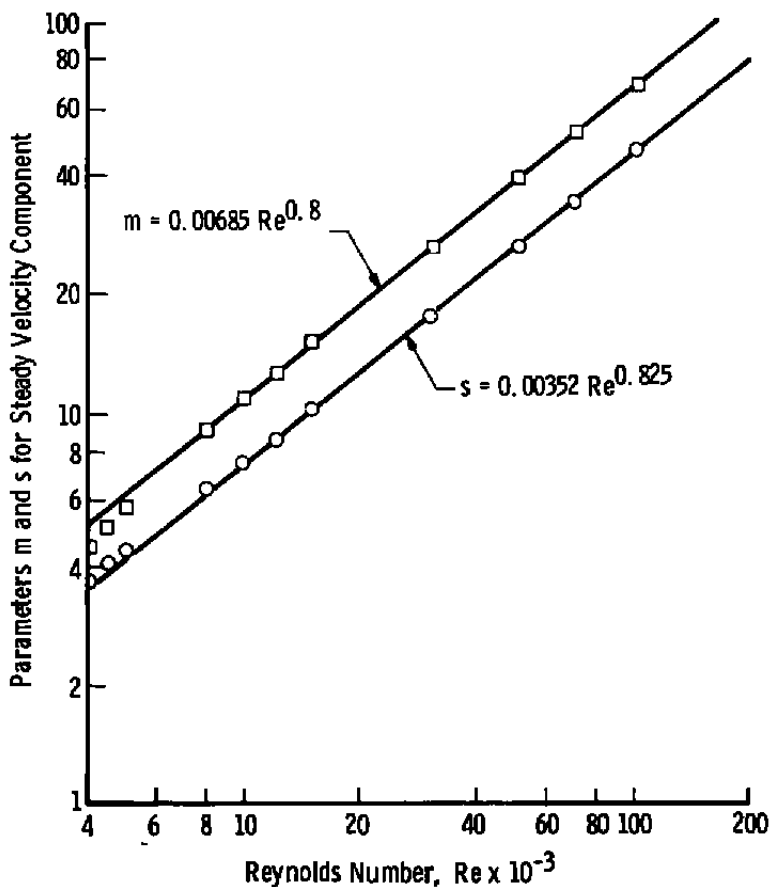


Figure 2. Variation of velocity profile parameters with Reynolds number.

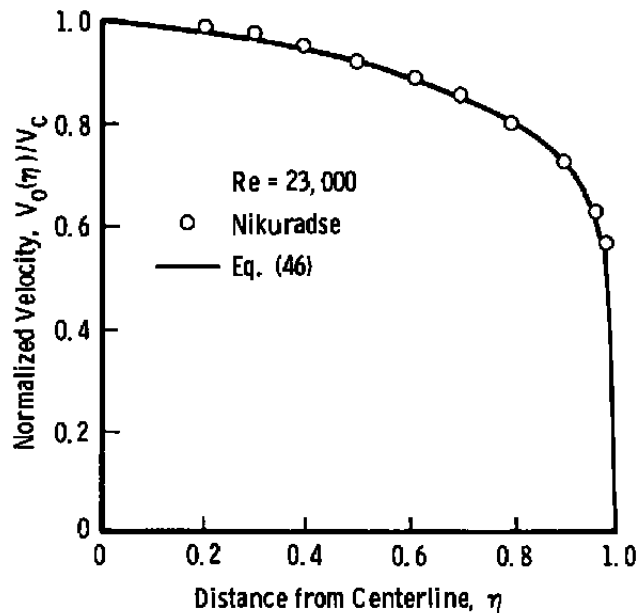


Figure 3. Comparison of theoretical and experimental velocity distributions in steady turbulent flow.

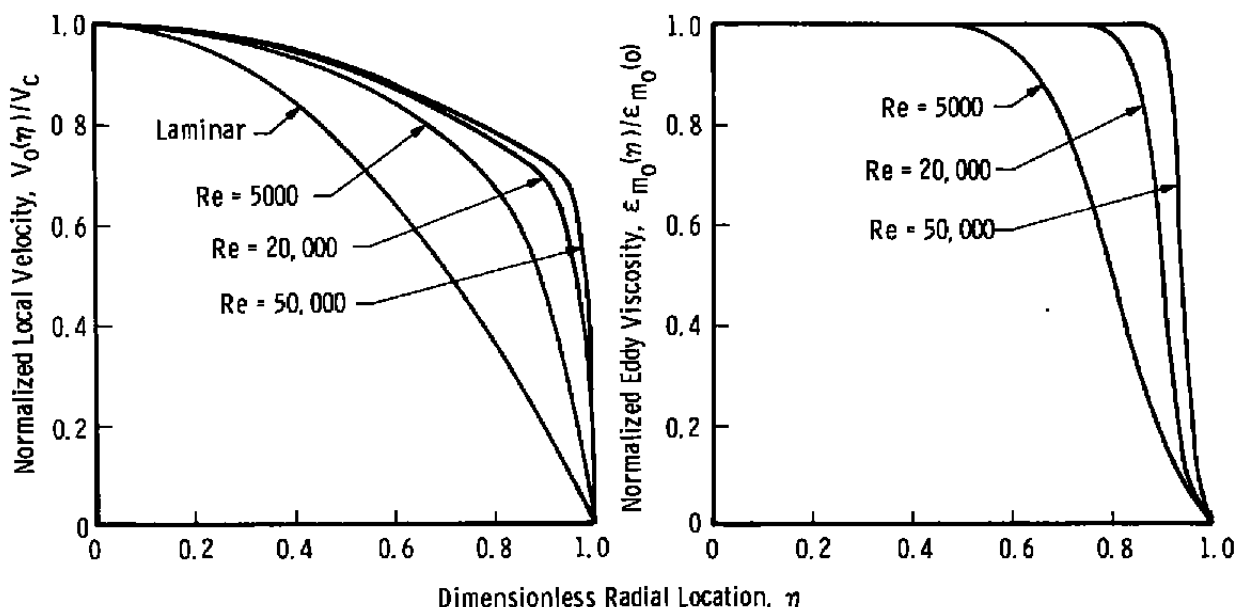


Figure 4. Velocity and eddy viscosity distributions in steady, fully developed flow in a tube.

on the basis of hot-wire studies that the exchange process was altered but presented no quantitative information. Mickelson and Lawrence (Ref. 15), on the other hand, showed that acoustic excitations affect the spectrum of turbulence only in the immediate vicinity of the exciting frequency. Recent experiments by Clamen and Menton (Ref. 7) show that pulsating flows with no mean motion begin to exhibit intermittent turbulent behavior when the harmonic Reynolds number ($Re_h = A Re_v$) exceeds 1,000 and are fully turbulent for $Re_h > 3,000$. None of these studies permits the exchange process to be modeled in detail although it is probable that turbulent exchange is increased in the presence of pulsations. In the absence of the required information, some insight into the influence of pulsation-induced turbulence can be obtained by assuming that the eddy diffusivity associated with the transient velocity field is spatially invariant. By analogy to the eddy viscosity distribution in steady flows (Fig. 4), this assumption should approximate the physical behavior if the vibrational and harmonic Reynolds numbers are large.

For $\epsilon_m/\nu = \text{constant}$, Eq. (51) becomes

$$f'' + \frac{1}{\eta} f' - i Re_v^* f = -\tilde{G}^* \quad (52)$$

where

$$Re_v^* = \frac{Re_v}{1 + \frac{\epsilon_m}{\nu}} \quad (53)$$

and

$$\tilde{G}^* = \frac{\tilde{G}}{\epsilon_m} \frac{1}{1 + \frac{\epsilon_m}{\nu}} \quad (54)$$

A particular solution to Eq. (52) is

$$f_p = -i \frac{\tilde{G}^*}{Re_v^*} \approx -i \frac{\tilde{G}}{Re_v} \quad (55)$$

The homogeneous form of Eq. (52) is a modified Bessel equation of order zero. Its solution is

$$f_h = C_1 I_0(i^{1/2} a^* \eta) + C_2 K_0(i^{1/2} a^* \eta) \quad (56)$$

where $a^* = \sqrt{Re_v}$ is commonly termed the frequency factor. The general solution to Eq. (52), then, is the sum of Eqs. (55) and (56). For the boundary condition $f(1) = 0$ and the constraint that $f(\eta)$ must be finite for all values of η , $0 \leq \eta \leq 1$, the general solution may be written as

$$f(\eta) = i \frac{\mathcal{Q}}{Re_v} \left\{ \frac{I_0(i^{1/2} a^* \eta)}{I_0(i^{1/2} a^*)} - 1 \right\} \quad (57)$$

It is convenient to express this result in an alternative form. First, it is noted that a modified Bessel function, $I_\nu(i^{1/2}x)$ may be expressed in terms of the Kelvin functions $\text{ber}_\nu x$ and $\text{bei}_\nu x$ by (Ref. 16)

$$I_\nu(i^{1/2}x) = \text{ber}_\nu x + i \text{bei}_\nu x \quad (58)$$

An equivalent form of Eq. (58) is the polar representation

$$I_\nu(i^{1/2}x) = M_\nu(x) \exp \left[i \theta_\nu(x) - \frac{\nu \pi}{2} \right] \quad (59)$$

where the modulus is

$$M_\nu(x) = \left[\text{ber}_\nu^2(x) + \text{bei}_\nu^2(x) \right]^{1/2}$$

and the phase is

$$\theta_\nu(x) = \tan^{-1} \frac{\text{bei}_\nu x}{\text{ber}_\nu x}$$

Substituting Eq. (57) into Eq. (50) along with the definition given by Eq. (59) gives

$$V_1(\eta, \tau) = \frac{\mathcal{Q}}{Re_v} \left\{ \sin \tau - \frac{M_0(a^* \eta)}{M_0(a^*)} \sin \left[\tau - \theta_0(a^* \eta) - \theta_0(a^*) \right] \right\} \quad (60)$$

Detailed discussion of this result will be deferred until Section 3.0, but two effects are readily apparent from the equation. First, the magnitude of the transient velocity is directly proportional to an attenuated value of the generalized amplitude. For a fixed value of \mathcal{Q} , high frequencies tend to diminish the effect of pulsations. Secondly, the fluid velocity is out of phase with the excitation, $\mathcal{Q} \cos \tau$, by an amount which varies with location in the tube. On the centerline of the tube, it is readily apparent that the phase lag approaches 90 deg.

2.5 PULSATIONS OF ARBITRARY WAVEFORM

In many cases of engineering significance, the forcing function, $\mathcal{F}(\tau)$, of Eq. (39) is a periodic function of greater complexity than the simple harmonic pulsation discussed above. If, however, the function is bounded and has a finite number of discontinuities in the interval $P = 2\pi/\omega$, it is known that a Fourier trigonometric series will converge to the value of the forcing function in the interval. Consequently, many practical waveforms can be represented by a Fourier series in the various harmonics of the basic frequency, ω . (Turbulent fluctuations, however, are aperiodic and require a Fourier integral approach.)

Considering the approach of the preceding section, it is desirable to express the forcing function by the complex series

$$\mathcal{F}(\tau) = H_0 + 2 \sum_{n=1}^{\infty} H_n e^{int} \quad (61)$$

where

$$H_n = \frac{1}{P} \int_{C}^{C+P} \mathcal{F}(\tau') e^{-int'} d\tau' \quad (62)$$

In Appendix B it is shown that this expansion is a special case of the more general complex Fourier expansion. It applies for any $\mathcal{F}(\tau)$ which is real and satisfies the Dirichlet conditions. The limits of integration in Eq. (62) extend from an arbitrary point C of a cycle to the initial point of the succeeding cycle while the summation indices are harmonics of the basic frequency of the oscillation, $\omega = 2\pi/P$.

A form of the velocity field is sought which is consistent with Eq. (61). Accordingly, let

$$V(\eta, \tau) = V_0 + \sum_{n=1}^{\infty} V_n(\eta) e^{int} \quad (63)$$

Similarly, the correlation function may be written as

$$R_{uw} = -\frac{1}{\nu Re^*} \left[\epsilon_{m_0}(\eta) \frac{dV_0}{d\eta} + \epsilon_{m_1}(\eta) \frac{d}{d\eta} \sum_{n=1}^{\infty} V_n e^{int} \right] \quad (64)$$

Substitution of Eqs. (61), (63), and (64) into the axial momentum Equation, Eq. (39), leads to a separation of variables in which the following relations must be satisfied:

$$\frac{1}{\eta} \frac{d}{d\eta} \left[\eta \left(1 + \frac{\epsilon_{m_0}}{\nu} \right) \frac{dV_0}{d\eta} \right] + \mathcal{H}_0 = 0 \quad (65)$$

$$\sum_{n=1}^{\infty} \left\{ \frac{1}{\eta} \frac{d}{d\eta} \left[\eta \left(1 + \frac{\epsilon_{m_1}}{\nu} \right) \frac{dV_n}{d\eta} \right] - i n \text{Re}_v V_n + 2 \mathcal{H}_n \right\} e^{inx} = 0 \quad (66)$$

Equation (65) governs the mean fluid motion and is identical to Eq. (44) for $\text{Re}^* = \mathcal{H}_0/2$. Since the boundary conditions to be satisfied are $V_0(1) = 0$ and $V_n(1) = 0$, the solutions proposed in Section 2.4.1 for the mean motion are applicable here as well. For Eq. (66) to be valid at all times, it follows that each harmonic must obey a relation of the form

$$\frac{1}{\eta} \frac{d}{d\eta} \left[\eta \left(1 + \frac{\epsilon_{m_1}}{\nu} \right) \frac{dV_n}{d\eta} \right] - i n \text{Re}_v V_n = -2 \mathcal{H}_n$$

or

$$\left(1 + \frac{\epsilon_{m_1}}{\nu} \right) V_n'' + \frac{1}{\eta} \left(1 + \frac{\epsilon_{m_1}}{\nu} + \frac{\eta \epsilon_{m_1}'}{\nu} \right) V_n' - i n \text{Re}_v V_n = -2 \mathcal{H}_n \quad (67)$$

The similarity of Eqs. (67) and (51) is readily apparent, as is the observation that again a lack of information exists on the eddy diffusivity associated with the transient fluid motion. As before, the heuristic assumption will be made that the eddy viscosity, ϵ_{m_1} , is spatially invariant. The solution to Eq. (67) is then

$$V_n = \frac{2 i \mathcal{H}_n}{n \text{Re}_v} \left\{ \frac{\frac{M_n(a_n^* \eta)}{M_0(a_n^*)} - e^{i[\theta_0(a_n^* \eta) - \theta_0(a_n^*)]}}{1 - 1} \right\} \quad (68)$$

where

$$a_n^* = \sqrt{\frac{n Re_v}{1 + \frac{\epsilon_m}{\nu}}} \quad (69)$$

9

Introducing Eqs. (68) and (46) into (63) completely specifies the velocity field in the tube at any time. For computational purposes it is expedient to compute the elements of Eq. (63) individually and sum the results. Additional savings in computational time are obtained if the various coefficients can be related to the coefficients of a Fourier trigonometric series (see Appendix B) so that a Fast Fourier Transform (FFT) algorithm (Ref. 17) may be used. With this in mind, note that Eq. (62) may be rewritten as

$$2 \mathcal{Y}_n = A_n - i B_n \quad (70)$$

where

$$A_n = \frac{2}{P} \int_0^P f(\tau') \cos n\tau' d\tau' \quad n = 0, 1, 2, \dots \quad (71)$$

and

$$B_n = \frac{2}{P} \int_0^P f(\tau') \sin n\tau' d\tau' \quad n = 1, 2, \dots \quad (72)$$

From Eq. (70) and DeMoivre's relation

$$e^{ix} = \cos x + i \sin x$$

it can be shown by a straightforward substitution that the real part of the n^{th} harmonic of the velocity may be expressed as

$$\text{Re} \left[V_n(\eta) e^{inx} \right] = \frac{1}{n Re_v} \left\{ \frac{M_0(a_n^* \eta)}{M_0(a_n^*)} \left[A_{n_1}(\tau) \cos \Delta \theta_n - A_{n_2}(\tau) \sin \Delta \theta_n \right] \right\} \quad (73)$$

where

$$A_{n_1}(\tau) = B_n \cos n\tau - A_n \sin n\tau \quad (74)$$

$$A_{n_2}(\tau) = A_n \cos n\tau + B_n \sin n\tau \quad (75)$$

$$\Delta \theta_n = \theta_o(a_n^* \eta) - \theta_o(a_n^*) \quad (76)$$

An equivalent result to Eq. (73) is

$$\begin{aligned} \operatorname{Re} \left[V_n(\eta) e^{in\tau} \right] &= \frac{A_n}{n \operatorname{Re} v} \left\{ \sin n\tau - \frac{M_n(a_n^* \eta)}{M_n(a_n^*)} \sin \left[n\tau + \theta_o(a_n^* \eta) - \theta_o(a_n^*) \right] \right\} \\ &= \frac{B_n}{n \operatorname{Re} v} \left\{ \cos n\tau - \frac{M_n(a_n^* \eta)}{M_n(a_n^*)} \cos \left[n\tau + \theta_o(a_n^* \eta) - \theta_o(a_n^*) \right] \right\} \quad (77) \end{aligned}$$

As in the case of simple harmonic oscillations the amplitude of the transient component is attenuated at high frequencies, and phase lags exist that depend on radial location and frequency. A more detailed discussion of these results and, in particular, the effect of waveform on the solution, is presented in Section 4.0.

3.0 THE VELOCITY FIELD FOR SIMPLE HARMONIC PULSATIONS

The response of the fluid to a pulsation of the form described by Eq. (40) is simply the sum of Eqs. (46) and (60). Although this sum is a closed form analytic solution of the transient Reynolds equation for fully developed flow, the complexity of the equations and the number of auxiliary relations to be solved make its evaluation practical only by use of a computer. A program identified as PULSAT has been written for an IBM 370/165 digital computer to evaluate the velocity field in fully developed, laminar or turbulent, steady or pulsating flows of simple harmonic waveform.

3.1 THEORETICAL RESULTS

The radial distribution of velocities in a flow with a mean Reynolds number of 10,000 is shown in Fig. 5 for several times during a cycle of pulsation. At $\tau = 0$, the velocity profile is

seen to correspond to steady flow in a tube at this Reynolds number except for a thin layer of fluid near the tube boundary where the velocity increases rapidly to a value in excess of that observed on the centerline before decaying to zero at the wall. It should be recalled that, due to the quasi-steady nature of the solution, $\tau = 0$ corresponds to the start of a cycle but *not* to the initial time at which pulsations are induced. With increasing values of τ the magnitude of the velocity increases until the maximum value is obtained at $\tau = 90$ deg. The magnitude and extent of the velocity increases near the wall are also seen to vary with time during a cycle. After the maximum velocity is obtained, the velocity is seen to decrease until the minimum

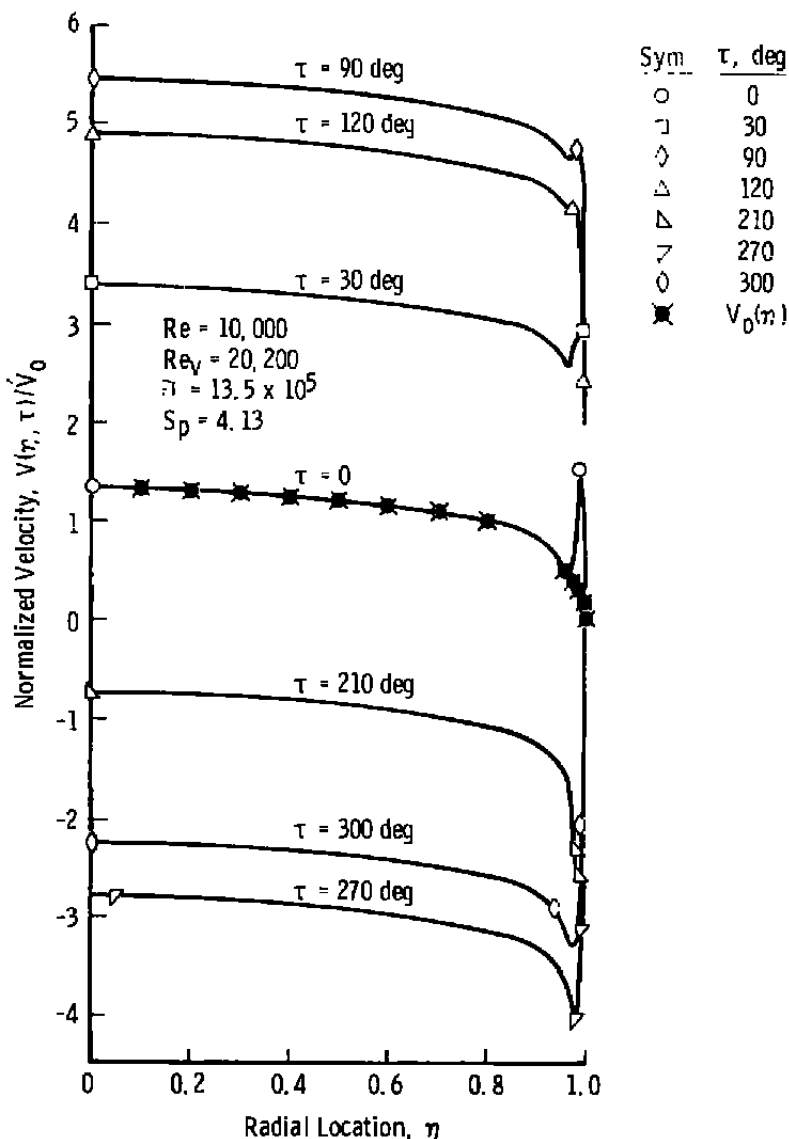


Figure 5. Temporal variation of local velocity for harmonic forcing function.

values are obtained at $\tau = 270$ deg. It is apparent and will be seen in later results that during a cycle there are times at which the core velocities are positive while near the wall the velocity is negative.

Since the forcing function is a maximum at $\tau = 0$ and a minimum at $\tau = 180$ deg, the centerline velocity lags the forcing function by 90 deg. This behavior was anticipated on the basis of Eq. (60), which shows that the phase lag depends on both the frequency parameter, $a^* = \sqrt{Re_v}$, and the radial location, η . In Fig. 6, the phase lag is plotted as a function of η for two vibrational Reynolds numbers. The fluid phase behavior is of significance in any application in which a secondary response to the forcing function (such as particle dynamic effects, flow-induced vibrations, etc.) are of importance. A striking example is that some techniques proposed for sizing particles contained in a flow (Ref. 18) relate the particle drag to pressure pulsations imposed upon the flow. Failure to properly account for the fluid behavior could lead to serious errors in such determinations.

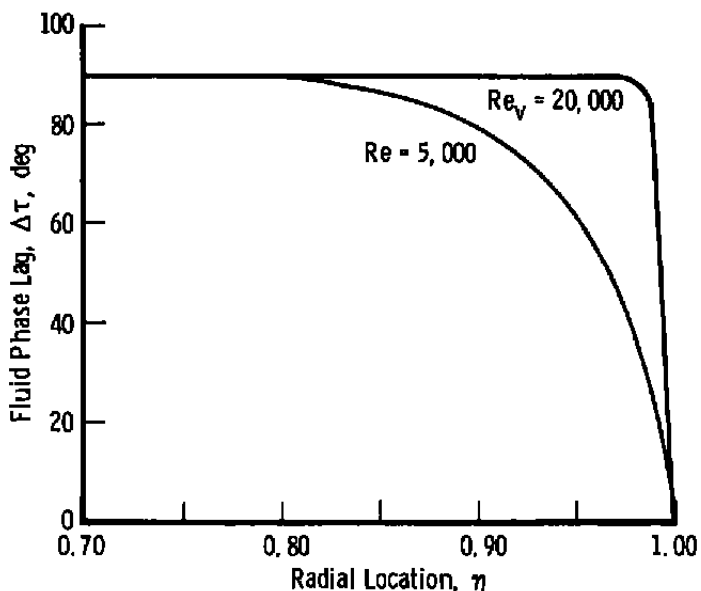


Figure 6. Phase lag of the velocity for a simple harmonic pulsation.

The effect of the mean throughflow Reynolds number on the velocity observed at various times during a cycle in which pulsations are vibration-induced is illustrated in Fig. 7. As would be expected, the gross effect of increasing Reynolds number is to diminish the overall influence of the pulsation. Indeed, for a fixed value of A and Re_v , the transient component of velocity, Eq. (60), is independent of Reynolds number provided the turbulent structure is unaltered or varies independently of Reynolds number.

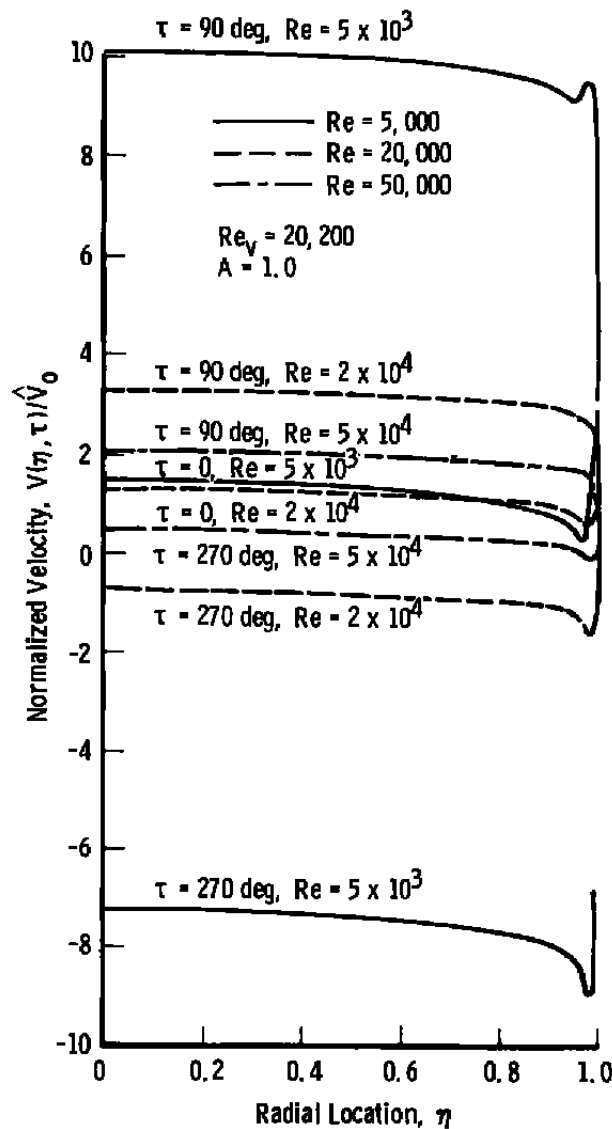


Figure 7. Temporal variation of velocity for several Reynolds numbers.

Specifying the amplitude of the vibration at the tube boundary, A , is not, however, equivalent to specifying a constant generalized amplitude, as may be seen from Eq. (41). Since the transient velocity component profiles normalized with respect to the centerline values $V_1(0, \tau)$ are identical for all Reynolds numbers and vibrational Reynolds numbers, the effect of amplitude may be studied by simply considering the magnitude of the centerline velocity. This evaluation is facilitated if the radial distribution function of Eq. (50) is written as

$$f(\eta) = f_r(\eta) + i f_i(\eta) \quad (78)$$

where, from Eq. (57),

$$f_r(\eta) = \frac{Q}{Re_v} \left\{ \frac{M_o(a^* \eta)}{M_o(a^*)} \sin \left[\theta_o(a^*) - \theta_o(a^* \eta) \right] \right\} \quad (79)$$

and

$$f_i(\eta) = - \frac{Q}{Re_v} \left\{ 1 - \frac{M_o(a^* \eta)}{M_o(a^*)} \cos \left[\theta_o(a^*) - \theta_o(a^* \eta) \right] \right\} \quad (80)$$

The transient velocity component is then, simply,

$$V_1(\eta, \tau) = f_r \cos \tau - f_i \sin \tau \quad (81)$$

Various authors (Refs. 3 and 6) define the strength of pulsation as the ratio of the maximum velocity amplitude on the centerline of the tube to the mean throughflow velocity. In the present notation, this may be written as

$$S' = \frac{V_1(0, \tau^*)}{\hat{V}_o} \quad (82)$$

where τ^* is the time at which the maximum value of the transient occurs. From Eq. (81), $V_1(\eta, \tau)$ attains a maximum value for

$$\tau^* = \tan^{-1} \frac{f_i(\eta)}{f_r(\eta)}$$

The corresponding maximum centerline value can be obtained as (Ref. 4)

$$V_1(0, \tau^*) = \frac{\hat{Q}}{Re_v} \left[1 - 2 \frac{\cos \theta_o(a^*)}{M_o(a^*)} + \frac{1}{M_o^2(a^*)} \right]^{1/2} \quad (83)$$

For all but extremely low frequencies, the modulus $M_o(a^*)$ is extremely large, and the bracketed term in Eq. (83) approaches unity. From the definition of the friction Reynolds number and the mean throughflow Reynolds number the strength of pulsation is then

$$S' = \frac{2 \hat{Q} Re^*}{Re Re_v} \quad (84)$$

From Eq. (41) it is readily apparent that a constant pulsation strength is obtained in a vibrating tube ($A_p = 0$) for

$$S = \frac{A Re_v}{Re Re^*} \quad (85)$$

Similarly, the strength of pulsation for pressure-induced oscillations ($A = 0$) is

$$S = \frac{2 A_o Re^*}{Re Re_v} \quad (86)$$

Since the friction Reynolds number is related to the mean Reynolds number through the Fanning friction factor (see Section 2.2), one of the parameters can be eliminated from these equations. For example, for turbulent flow in a pipe (Ref. 12),

$$C_f \approx 0.046 Re^{-1/5} \quad (Re < 10^5)$$

Thus

$$S = 13.19 \frac{A Re_v}{Re^{1.9}} \quad (87)$$

for vibrations, and

$$S = 0.1517 \frac{A_p}{Re_v Re^{0.1}} \quad (88)$$

for pressure pulsations. It follows, therefore, that the effect of pulsations is diminished at large Reynolds numbers for either pressure-induced or vibration-induced oscillations although this trend is much more pronounced in the latter case. On the other hand, high frequencies increase the pulsation strength for vibrations but attenuate the effect of pressure pulsations.

The effect of frequency on the velocity profile in the vicinity of the tube wall is shown for several vibrational Reynolds numbers in Fig. 8. Since these profiles, as well as the centerline

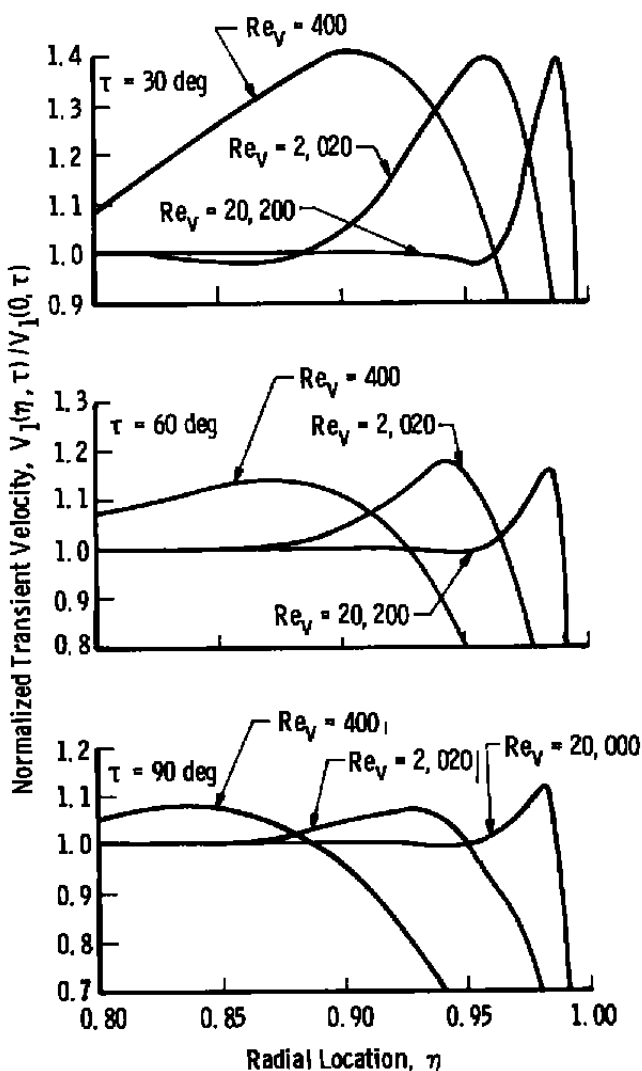


Figure 8. Influence of vibrational Reynolds number on transient velocity component.

velocity (Fig. 9) are, ostensibly, independent of the mean flow characteristics, the trends are applicable for all Reynolds numbers. It is seen that as the frequency is increased the local maximum "moves" nearer the wall. This phenomenon has been termed the "annular"

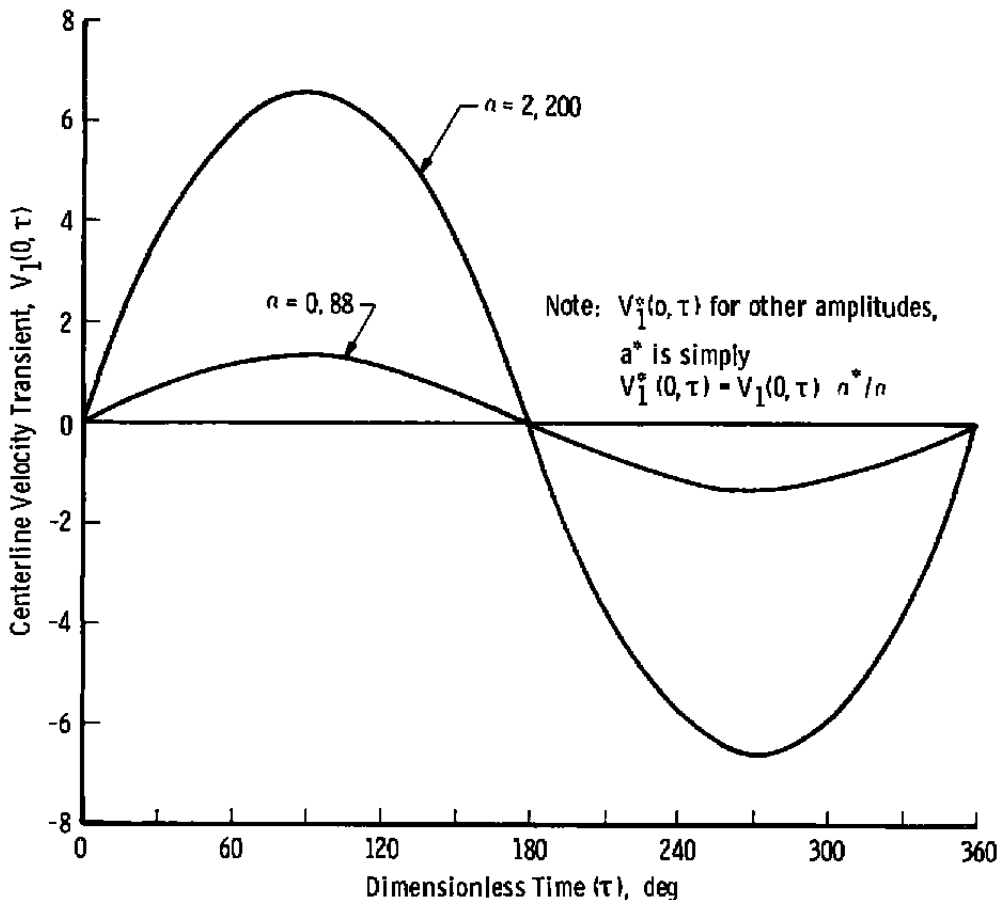


Figure 9. Temporal and amplitude dependence of transient centerline velocity.

effect and has long been of interest to fluid dynamicists (Refs. 1 and 9). The actual location and magnitude of the maximum during a cycle is, however, a function of time, as could be inferred from Figs. 5 and 6. To illustrate the frequency dependence of the maximum velocity location, it is useful to consider the root-mean-square (rms) value of the transient velocity. From Eq. (81), this is simply

$$\langle V_1^2 \rangle^{\frac{1}{2}} = \sqrt{\frac{f_r^2 + f_1^2}{2}} \quad (89)$$

The variation of the rms velocity is shown in Fig. 10 for a range of vibrational Reynolds numbers at a mean flow of $Re = 10^4$. It is seen that, for this vibration-induced example, the rms velocities increase by nearly three orders of magnitude when the frequency is varied by a factor of 20. (Note that for water in a 1-in.-radius tube, the corresponding circular

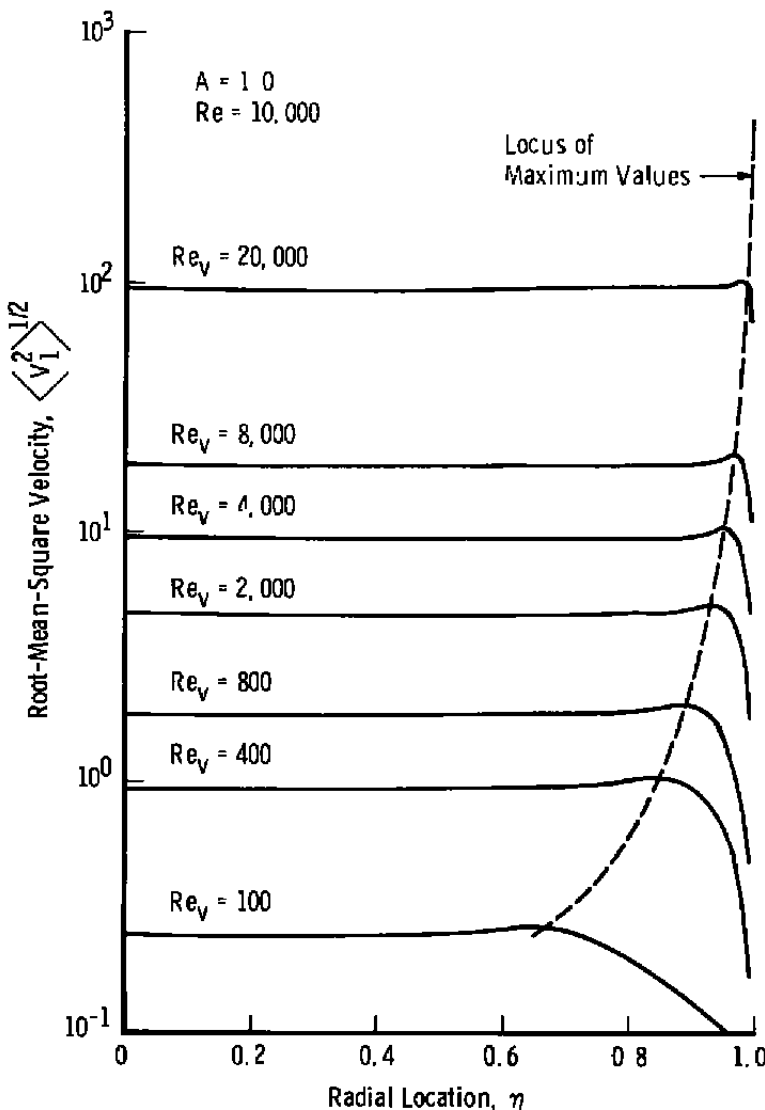


Figure 10. Effect of vibrational Reynolds number on RMS velocity component.

frequencies are 0.1 Hz at $Re_v = 100$ and 20 Hz at $Re_v = 20,000$. For air, $Re_v = 100$ implies that $f = 0.4$ Hz.) The annular effect is clearly seen, and the maximum velocity location, η^* , is very near the wall at large values of Re_v (Fig. 11). It can be shown, moreover (Ref. 19), that

$$\eta^* = 1 - \frac{3.25}{Re_v^*} \quad (90)$$

This result is of importance in calculations of pulsating flow characteristics since (1) important details of the flow may be lost if the computational grid is not varied as the wall is approached, and (2) alterations of the turbulent exchange process may be related to the location of these maxima (Ref. 4).

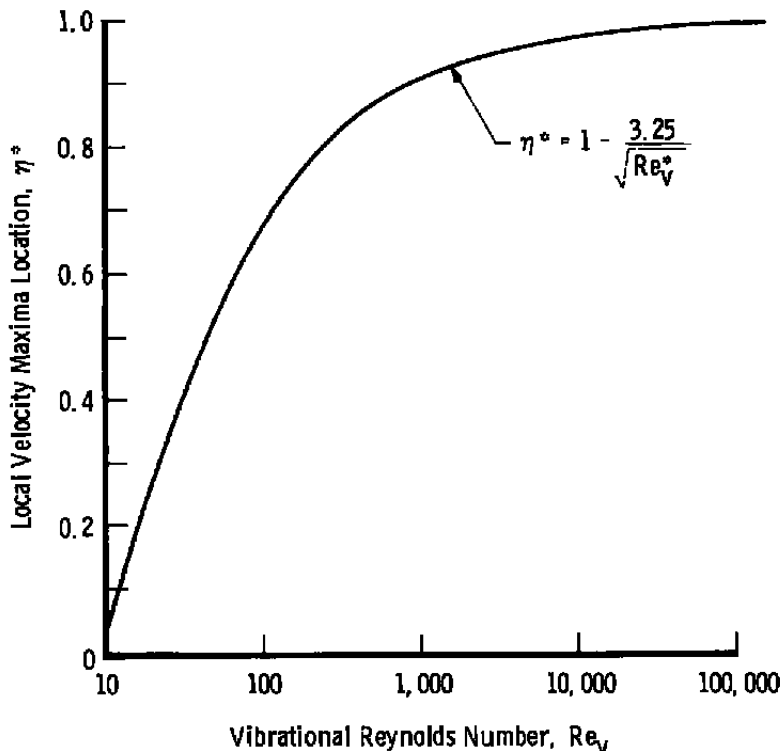


Figure 11. Variation of transient component maximum value location with frequency.

Both the analysis and the PULSAT program allow the determination of the velocity profile for the case where a constant eddy viscosity is associated with the velocity transient. While decidedly heuristic, the assumption leads to some interesting results, as may be seen in Fig. 12. The velocity profiles shown during the first half-cycle of a pulsation have been computed on the basis that (1) only molecular diffusion occurs ($\epsilon_{m1} = 0$) and (2) the turbulent diffusivity is equal to the spatial average of the eddy viscosity associated with the mean flow, $\epsilon_{m1} = \widehat{\epsilon_{m0}}$. A decided effect of $\epsilon_{m1} \neq 0$ is observed at all times. In general, since the governing parameter for the altered case is

$$Re_v^* = \frac{Re_v}{\frac{\epsilon_{m1}}{1 + \frac{\nu}{\epsilon_{m1}}}}$$

the solution behaves as though it corresponds to an $\epsilon_{m1} = 0$ flow at lower frequencies. The phase shift, moreover, depends on $Re_v^{1/2}$, and thus events occur at different times in the cycle than would be expected if alteration of the diffusion mechanisms were not present.

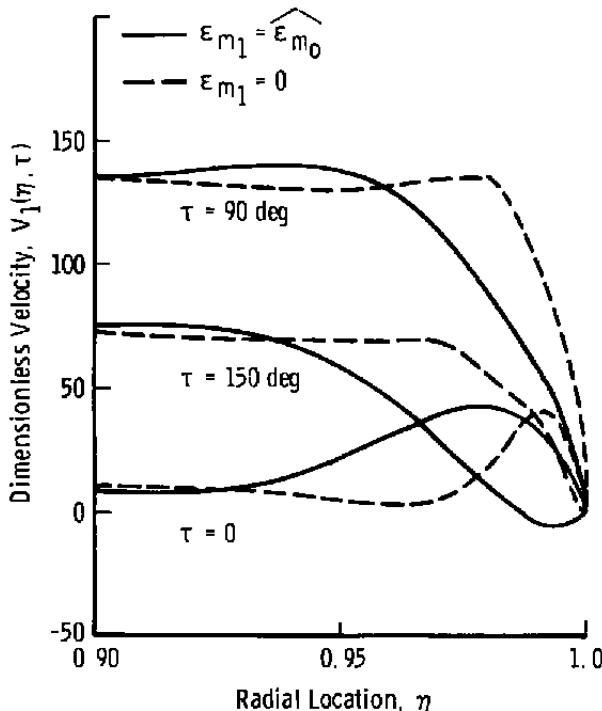


Figure 12. Near-wall velocity profiles for turbulent exchange modification.

3.2 COMPARISONS WITH EXPERIMENT

Data on the detailed variation of the velocity field in pulsating flows are extremely limited although considerable experimental information on the effect of pulsations on heat transfer exists (Ref. 8). Richardson (Refs. 1 and 20) measured the rms velocity field in a circular tube in the absence of a mean flow component and identified the annular effect discussed earlier. Additional hot-wire studies were made by Bogdonoff (Ref. 6) and Mohajery (Ref. 21) for air flows at mean Reynolds numbers in the range from 50,000 to 100,000. Both investigations showed that pressure pulsations altered the eddy viscosity distribution in the flow, but whereas Mohajery concluded the effect was not appreciable at any radial location in the tube, Bogdonoff observed significant increases in eddy viscosity near the tube wall. In the latter study, however, the author observed that this was a tentative result since it was difficult to compensate for probe blockage and compressibility effects. Recently, Clamen and Menton (Ref. 7) used a hydrogen bubble technique to study water flows in a vibrating tube from $Re = 0$ to $Re = 2,900$ for a range of amplitudes and

frequencies. Since these data conform better to the incompressible assumption of the present analysis, the comparisons that follow will be based on their data.

Figure 13a compares the velocity distribution measured in a purely oscillatory flow ($Re = 0$) to the present theory for several times during a cycle. Clearly the theory and experiment are in good agreement at the times shown with the exception of the small amplitude oscillation for $\tau = 30$ deg. Since the hydrogen bubble technique requires synchronization of a flash photograph with a particular cycle time, it is possible that the discrepancy is due to a timing error. (For $\omega = 1.2$ Hz, a 0.1-sec error would readily account for the difference.) In Fig. 13b, theory and experiment are again compared for a mean flow Reynolds number in the laminar flow regime ($Re = 1,535$). For both cases the agreement is excellent.

A final comparison is made in Fig. 14 for a turbulent mean flow at $Re = 2,900$. At $\tau = 0$, the present theory represents the flow accurately and represents a decided improvement over a laminar flow theory used in Ref. 7. For later times in the cycle, however, the turbulent theory grossly overpredicts the measured velocity. While this may be due to a deficiency of the theory, it is more likely due to one or more experimental factors. Clamen and Menton

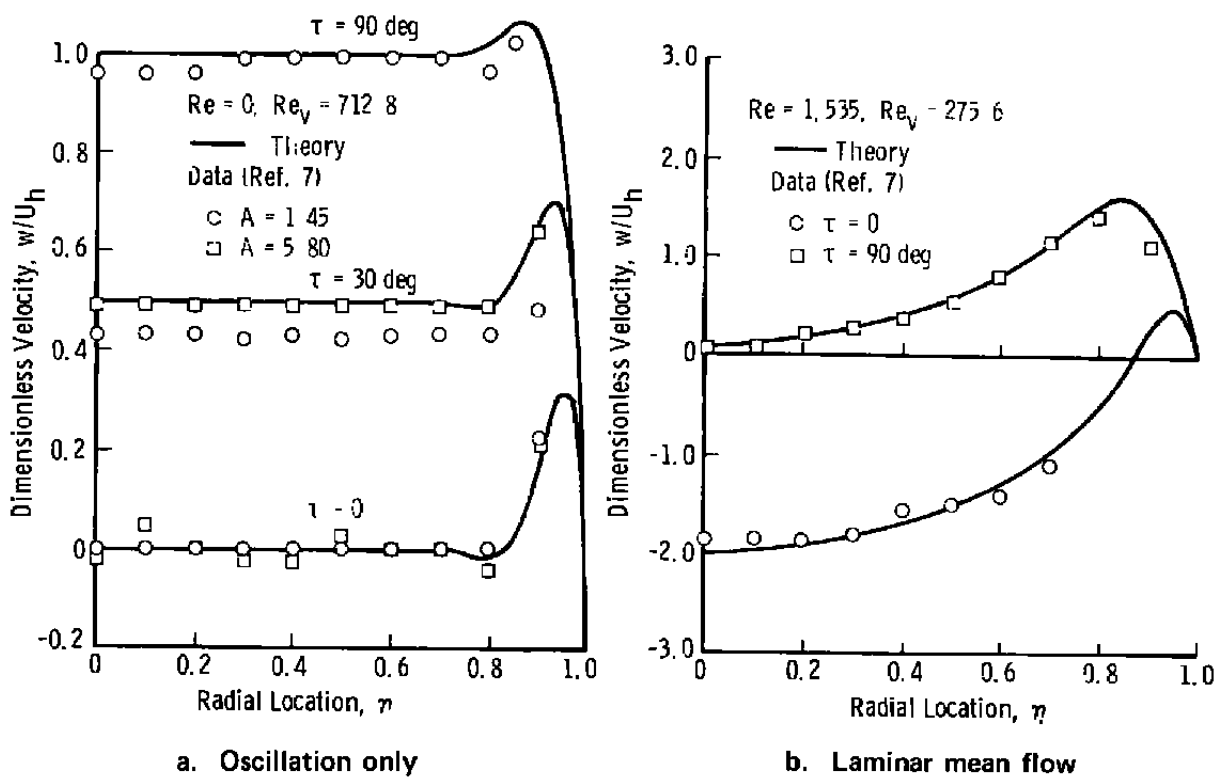


Figure 13. Comparison of experiment and theory in laminar pulsating flow.

note that at turbulent Reynolds numbers the flow was "highly disturbed" so that the photographic representation of the velocity profile was smeared. Under those conditions the hydrogen bubble technique shows a range of velocities so that the values obtained are highly dependent upon the fashion in which the data were reduced. The possibility of timing errors also exists, as was noted in the discussion of Fig. 13a. For $\omega = 1.12$ rad/sec, the displacement in centerline velocity from the theory could be accounted for by a time delay of 0.4 and 0.2 sec for $\tau = 90$ and 210 deg, respectively. While such shifts seem excessive, some credence is lent to the possibility by comparing the theoretical results for $\tau = 60$ deg to the data for $\tau = 90$ deg. The agreement is excellent for $\eta \leq 0.80$.

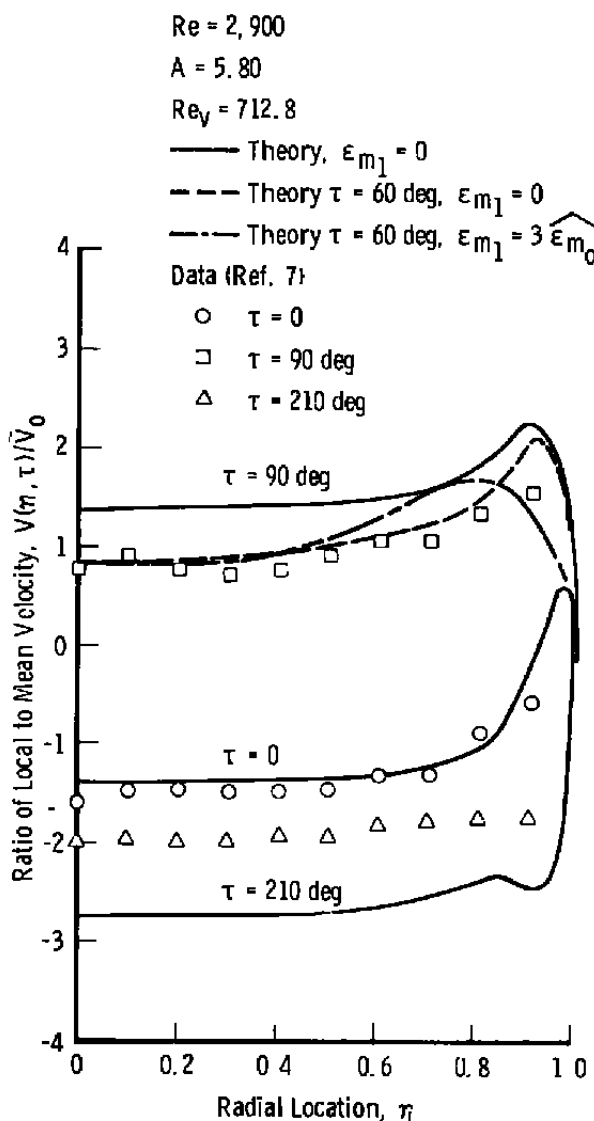


Figure 14. Comparison of experiment and theory in turbulent pulsating flow.

Since the model developed in Section 2.4 allows the investigation of a uniform alteration of the turbulent structure of the flow, such a comparison is made in Fig. 14. Clearly the assumption that $\epsilon_{m1} = 0$ is adequate at $\tau = 0$. At $\tau = 90$ deg (or 60 deg), however, $\epsilon_{m1} = 0$ leads to an overprediction of the data obtained near the wall. By letting $\epsilon_{m1} = 3\hat{\epsilon}_{m0}$, the velocity profile is damped relative to the undisturbed ($\epsilon_{m1} = 0$) profile for the wall region. The results are in error at intermediate locations $0.4 \leq \eta \leq 0.85$, however, so that an assumption of $\epsilon_{m1} = \text{constant}$ fails to predict the velocity distribution across the tube. From these limited data it appears that an accurate model of the alteration of turbulence structure must take into account the radial variation of the exchange coefficient.

4.0 THE VELOCITY FIELD FOR ARBITRARY WAVEFORMS

The analysis of Section 2.5 shows that the response of the fluid velocity to a forcing function of arbitrary waveform can be obtained by expanding the function in a complex Fourier series. Each harmonic of the transient velocity can then be obtained in terms of the various harmonics of the pressure disturbance. The amplitude of the velocity harmonics is determined by the Fourier coefficients required to describe the forcing function. A computer program (ARBPULSAT) for evaluating the velocity response has been written for performing such calculations. The results of computations performed via ARBPULSAT for several waveforms are described in the remainder of this section. No attempt has been made to comprehensively study the effect of waveform on the velocity distribution in a tube, but such studies are within the capabilities of the program.

4.1 EFFECT OF WAVEFORM

To study the possible influence of waveform upon the velocity distribution in pulsating flows, four different types of symmetric waves were considered. In each case, the initial and final third of a cycle were considered to be at a constant pressure while the pressure varied in the central portion of a cycle to produce (1) an instantaneous pressure change followed by a later instantaneous decay, (2) a linear rise followed by later linear decay, (3) a linear rise to a maximum value followed immediately by a linear decrease, and (4) a half-cycle sinusoidal variation from the initial pressure. These pressure variations will be called, respectively, (1) a square wave, (2) a trapezoidal wave, (3) a triangular wave, and (4) a sinusoidal wave in the following discussion.

Figure 15 shows the four waves which have been chosen so that in every case the mean pressure coefficient over a cycle corresponds to a time-averaged Reynolds number of 10^4 . Three amplitudes are shown in each figure, corresponding to peak-to-undisturbed pressure amplitudes of $\Omega_1/\Omega_0 = 100, 10$, and 1.5. Also shown in the figures are the Fourier series

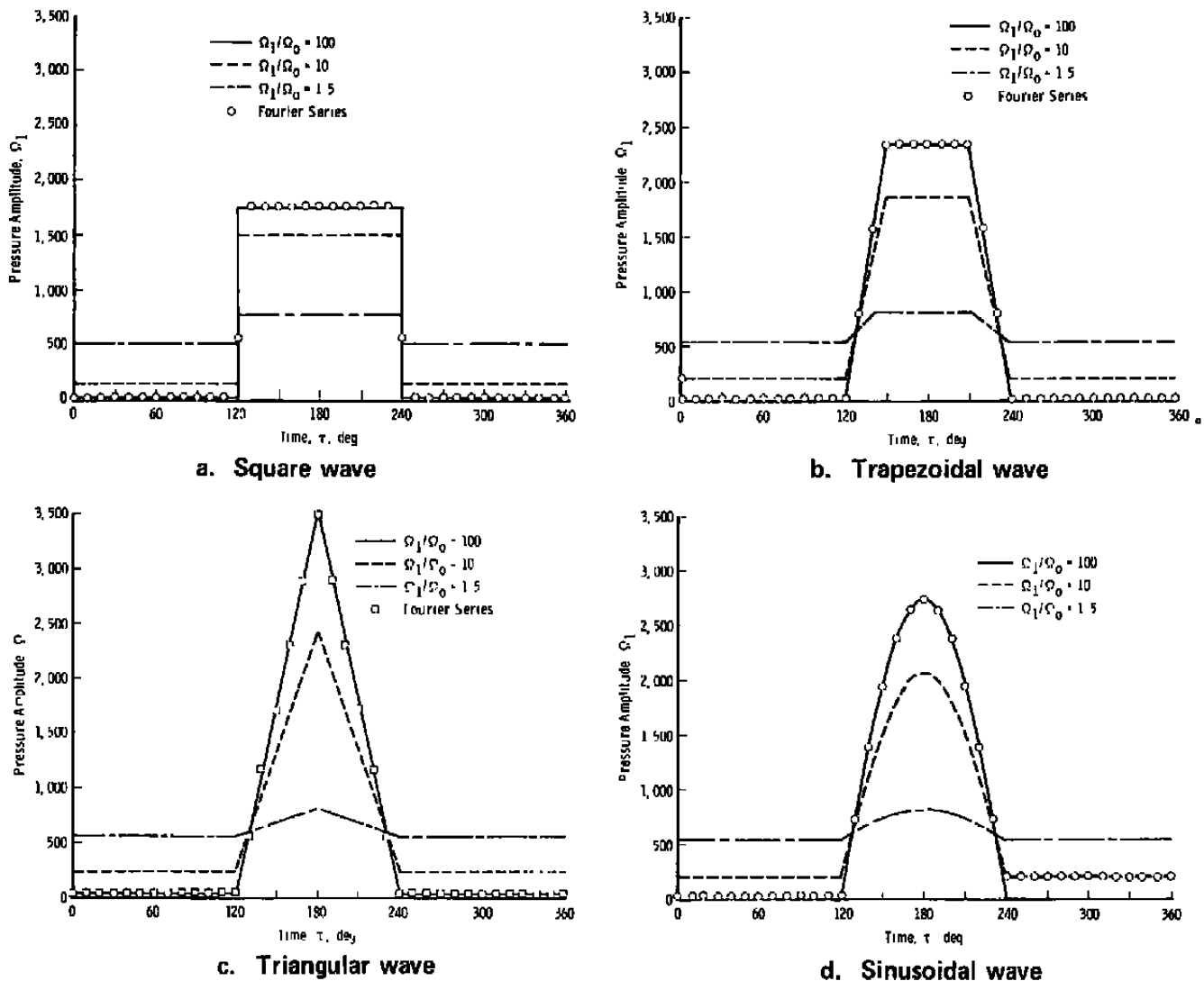


Figure 15. Symmetric forcing functions.

representations of the maximum amplitude wave for 2,048 (2^{11}) sine and cosine transforms, Eqs. (71) and (72). In all cases except the square wave the greatest departure of the computed value, Ω_F , from the input function, Ω_I , is $|\Omega_I - \Omega_F| < 1.0$. Since the minimum value of $\Omega_I \approx 25$, the error in representing the function at *any* point of the cycle is less than 4 percent and is typically better than 1 percent. Even better accuracy was obtained for lower values of the amplitude. The square wave is discontinuous at $\tau = 120$ and 240 deg and converges to $1/2 (\Omega_I + \Omega_o)$. Since the computed limit differs from this value by approximately $1/3$ it is clear that more coefficients are necessary to accurately describe the square wave in the immediate vicinity of the discontinuity. Since this is a localized error, it was not deemed of sufficient importance for the present study to warrant the additional computation time. (Since an FFT routine computes 2^n coefficients, the next possible choice was to double the number of coefficients used.)

The centerline transient velocities, $V_I(0, \tau) = \sum_{n=1}^N V_n(0, \tau)$, corresponding to the various waveforms are shown in Fig. 16. It is seen that regardless of waveform the centerline velocity histories are strikingly similar in both shape and amplitude. The observed "sawtooth" history was "somewhat unexpected and immediately raised a question as to whether the velocity field converges as rapidly as the series representation of the pressure transient. To explore this question it is useful to rewrite the forcing function as

$$\mathcal{F}(\tau) = \mathcal{F}_o + \mathcal{F}_I(\tau) \quad (91)$$

From Eqs. (61) and (70), then, one can write

$$\mathcal{F}_I(\tau) = \sum_{n=1}^{\infty} (A_n \cos n\tau - B_n \sin n\tau)$$

or

$$\mathcal{F}_I(\tau) = \sum_{n=1}^{\infty} C_n \cos(n\tau - \phi_n) \quad (92)$$

where

$$\left. \begin{aligned} C_n &= \sqrt{A_n^2 + B_n^2} \\ \phi_n &= \tan^{-1} \frac{B_n}{A_n} \end{aligned} \right\} \quad (93)$$

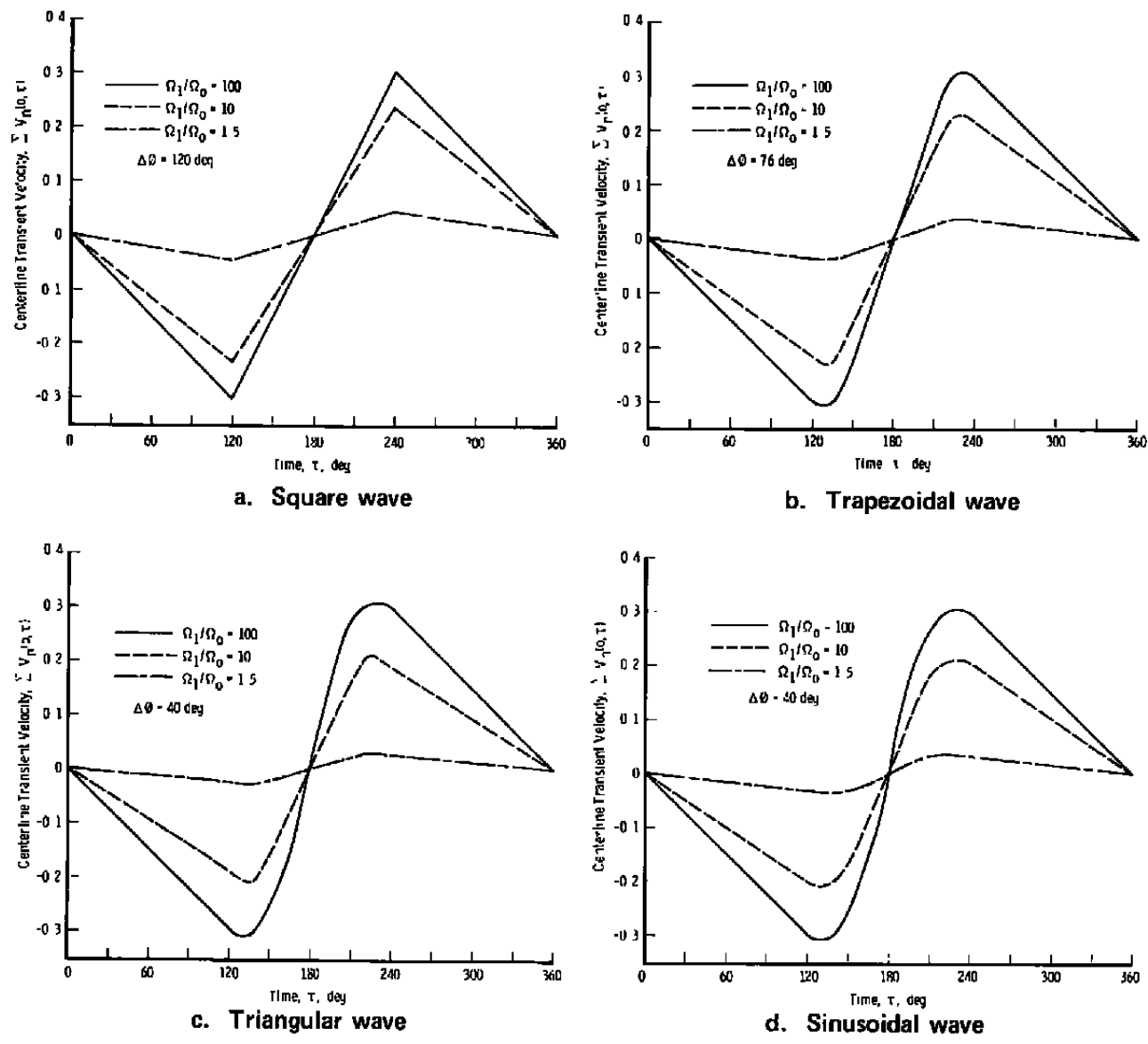


Figure 16. Centerline velocity response to symmetric waves.

On the centerline of the tube a similar result can be obtained if it is noted that $M_o(a_n^*) \gg 1$ for all but extremely low frequencies. Thus for $Re_v > 1$, Eq. (77) reduces to

$$V_1(0, \tau) = \frac{1}{Re_v} \sum_{n=1}^N \frac{C_n}{n} \sin(n\tau - \phi_n) \quad (94)$$

where C_n and ϕ_n are again given by Eq. (93). Clearly this result converges more rapidly than $F_1(\tau)$ so that for any identical number of terms the series for $V_1(0, \tau)$ will provide a better representation of the result than does that for $F_1(\tau)$. The expected rapid convergence of $V_1(\eta, \tau)$ is substantiated by Fig. 17 where the transient velocity corresponding to the partial sums, $\sum_{n=1}^N V_n(\eta, \tau)$ is compared to the result obtained for $N = 2^{11}$. Convergence was least rapid at $\tau = 120$ deg, which is where the pressure pulse representation was least accurate. Even in this "worst" case, the error for as few as 50 terms of the series was less than 0.65 percent and was virtually unaffected by radial location. It is concluded, therefore, that the velocity response observed on the centerline of the tube is an analytically valid result and is not due to any computational deficiency of the series representation.

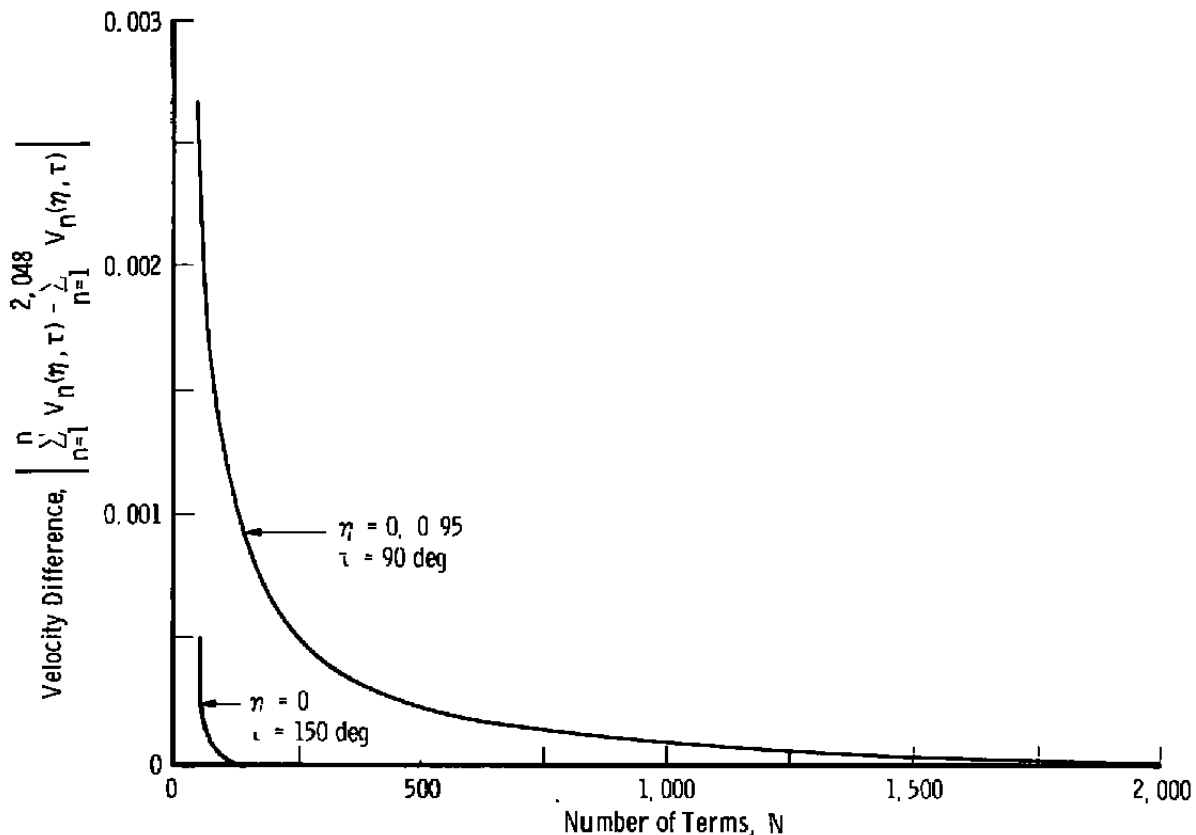


Figure 17. Convergence of transient velocity series for square wave excitation.

Some insight into the nature of the behavior of the centerline velocity is gained if the following integral representation is considered. Let $f(\tau)$ be an arbitrary function representing the variation of the pressure around the mean and consider the integral transform

$$g(\tau) = g_0 + a \int_0^\tau f(\tau) d\tau \quad (95)$$

If $f(\tau) = a \cos \tau$, a simple harmonic forcing function, Eq. (95) becomes

$$g(\tau) = g_0 + a \cos \tau \quad (96)$$

From Eq. (60), the fluid response on the centerline of the tube is then

$$V_1(0, \tau) = \frac{a \sin \tau}{Re_v} \quad (97)$$

so that the two results are identical if $\alpha = Re_v^{-1}$ and $g_0 = 0$. For the square wave, Fig. 15, $f(\tau) = 1/3(\Omega_0 - \Omega_1)$ for the initial and final portions of the cycle while for $2\pi/3 \leq \tau \leq 4\pi/3$, $f(\tau)$ is equal to $2/3(\Omega_1 - \Omega_0)$. The transform thus is of the form

$$g(\tau) = g_0 + \alpha K \tau \quad (98)$$

so that the centerline velocity varies linearly in each region of the pulse. The slope αK is, however, negative in the initial and final stages since Ω_0 is less than Ω_1 and is positive in the central region. The initial and final regions of the other waveforms also lead to a linearly decreasing function, but the response to the trapezoidal wave is parabolic during the linear rise and decay at the beginning and end of the pressure pulse. The triangular and sinusoidal waves, moreover, vary in a parabolic and cosinusoidal fashion, respectively, throughout the central region of the pressure pulse. The centerline transient velocity in a pulsating flow is accordingly given by a simple integral transform of the excitation for all waveforms. This behavior is observed at most radial locations in the tube so that molecular or turbulent diffusion is significant only in the vicinity of the tube wall. This is borne out by Fig. 18, where the fluid response to a square wave is shown at several radial locations in the tube. For $\eta < 0.90$, the velocity history is nearly independent of location, but near the wall significant departures both in the magnitude and waveform are observed. It is concluded, therefore, that viscous interactions become important near the boundary.

It is clear also that phase shifts are characteristic of the fluid response for the various waveforms studied. If one defines the phase shift as the time delay between the attainment of maximum pressure and velocity, a comparison of Figs. 15 and 16 shows that the

centerline phase lag varies from 40 deg for the sinusoidal variation to 120 deg for the square wave. It is apparent from Figure 18, moreover, that the phase lag is a function of radial location, as was shown for simple harmonic oscillations.

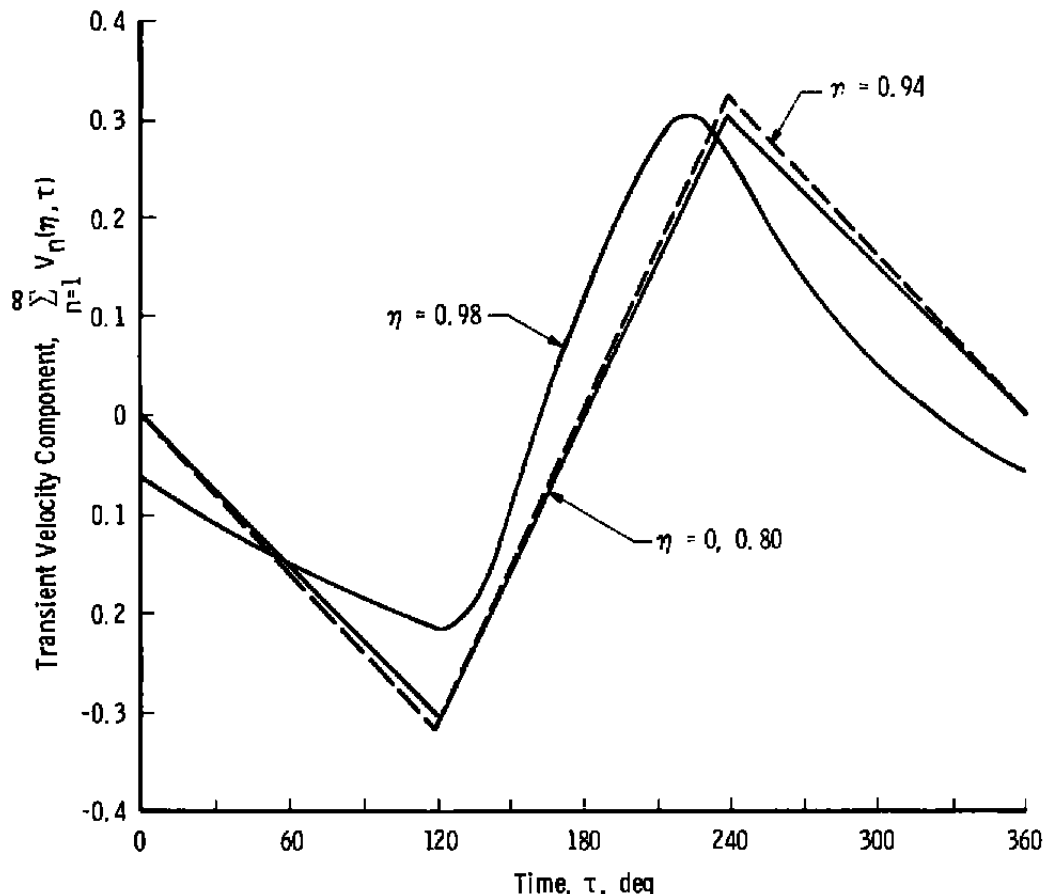


Figure 18. Comparison of velocity response to square wave at several radial locations.

The radial distribution of the transient velocity component for square and triangular waves is shown in Fig. 19. The annular flow phenomenon noted for harmonic oscillations is retained in both cases, and the magnitude of the maximum velocity is relatively insensitive to waveform for all excitations studied. A slight variation in the location of the maximum velocity point does result, however, for different forcing functions. Figure 20 illustrates the effect of vibrational Reynolds number on the velocity distribution obtained in response to a trapezoidal waveform. Clearly, increasing frequencies move the maximum velocity point nearer the wall and also decrease the amplitude of the velocity transient. Both effects were also observed in Section 3.0 for a simple harmonic oscillation. The lowest frequency case ($Re_v = 800$) compares the square and triangular wave results to those obtained for the trapezoid and emphasizes that for comparable amplitudes (Ω_1/Ω_0) the results are very insensitive to waveform.

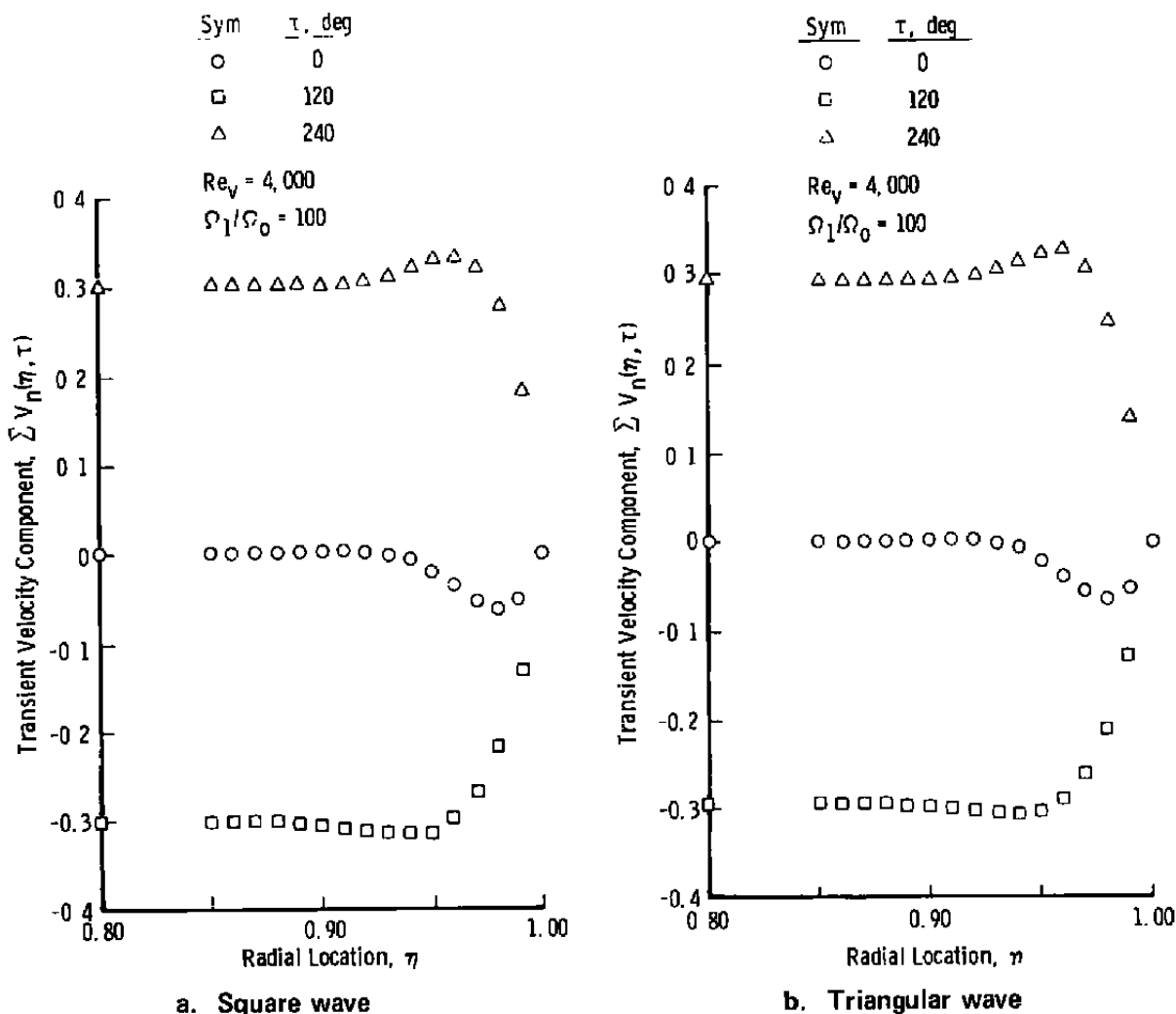


Figure 19. Velocity distribution for various times during a cycle.

It was noted in Section 3.1 that a convenient measure of the gross effect of a pulsation was afforded by the strength of pulsation, Eq. (82). The complex waveforms used in this section do not lend themselves to a simple evaluation of pulsation strength since each term of Eq. (94) achieves its maximum independently of the others when $\tau^* = 1/n \{[(2m-1)/2]\pi + \phi_n\}$. For the higher harmonics, then, τ^* is approximately equal to zero, but the phase lag of the lower frequencies must be evaluated individually to determine the time at which $V_1(0, \tau)$ is a maximum. This result is obviously dependent upon the waveform considered. For the waves considered in this section, however, the centerline velocities achieve a maximum at nearly the same time in the cycle and have nearly the same amplitude. Since, as can be seen in Eq. (94), only the lower harmonics contribute significantly to $V_1(0, \tau)$, it seems apparent that the fluid response is dictated only by the lower frequency components of the series.

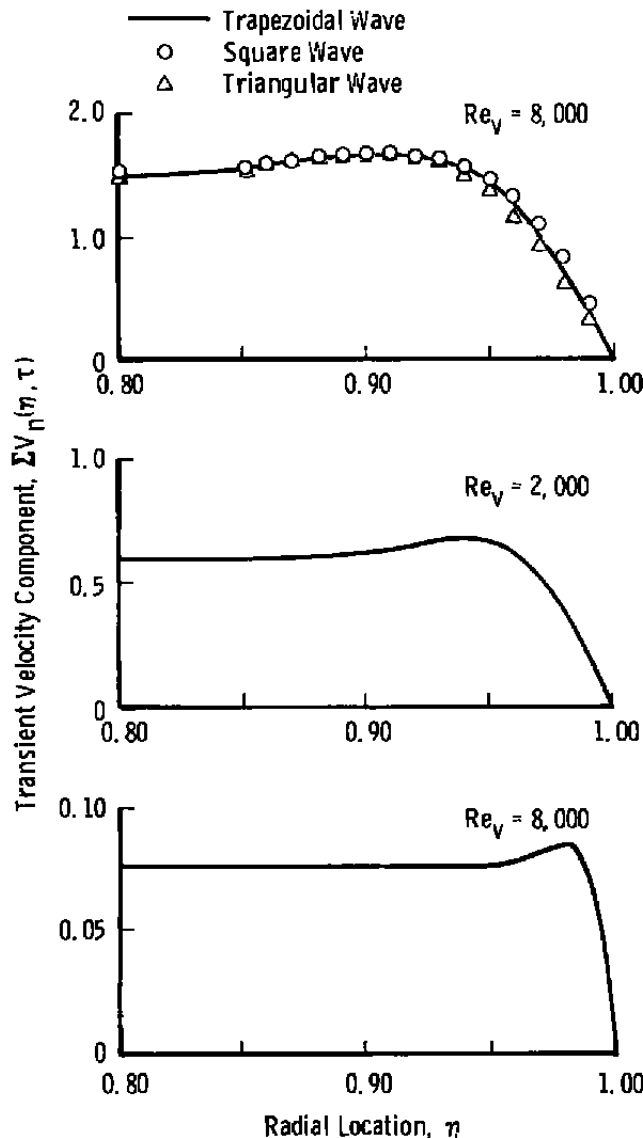


Figure 20. Effect of frequency on amplitude and radial distribution of transient velocity component.

4.2 Fluid Response to a Fluttering Valve

A final illustration of the utility of the computer program developed in this study is afforded by considering a basically steady flow that is perturbed at regular intervals. Such a situation could conceivably be caused by a fluttering valve or a faulty pressure regulator located in a flow system. Three illustrative cases are shown in Fig. 21 where a 0.1-sec pressure excursion occurs asymmetrically one, two, or three times per second. As in the preceding section, the mean flow Reynolds number is maintained at $Re = 10^4$; thus the relative amplitude of the pulse decreases as the repetition rate rises.

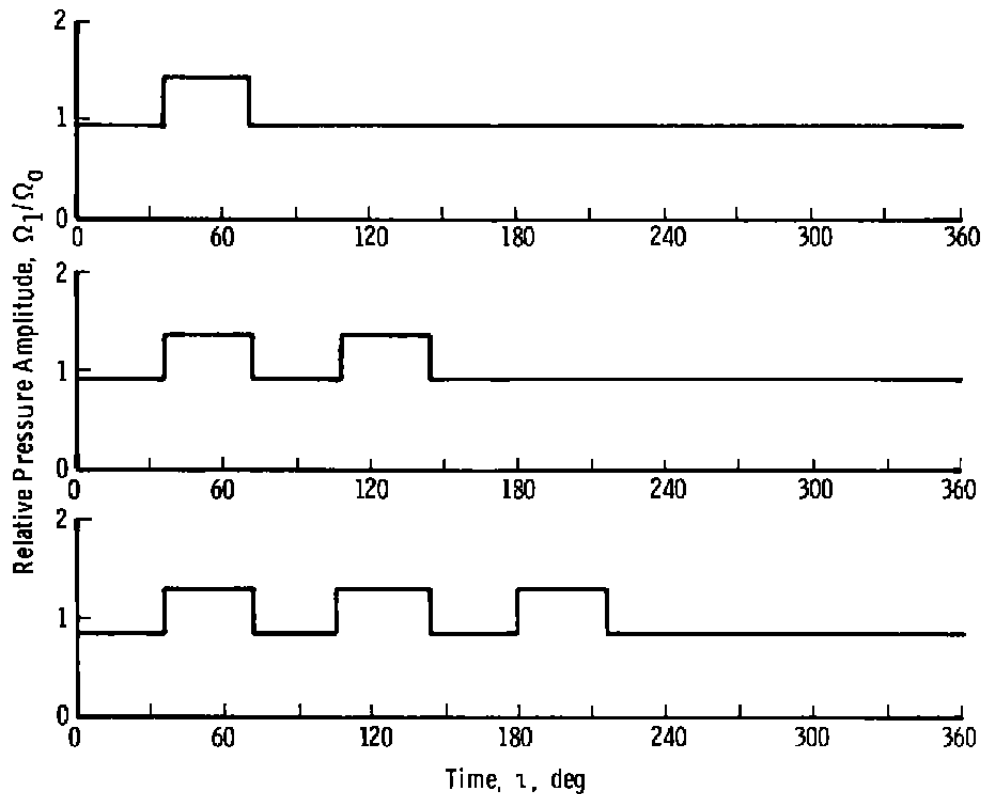


Figure 21. Asymmetric wave forms.

The fluid response on the centerline of the tube is shown in Fig. 22. For a single repetition the velocity history is similar to the square wave studied earlier, but as the repetitions are increased, the velocity history increases in complexity. For each additional repetition an additional local maximum (corresponding to the trailing edge of the added pulse) is obtained. Although the maximum value of the pressure coefficient has decreased with additional cycles, the absolute maximum centerline velocity increases, with the three-cycle result showing a 50-percent increase over that observed for a single cycle. This result implies that waveform *can* be influential in determining the fluid response to a pulsation.

The radial velocity distribution for the three cases is shown in Fig. 23 for a single time of the cycle ($\tau = 90$ deg). While all the velocity profiles exhibit a characteristic annular shape, significant variations in amplitude are obtained for differing repetition rates. It is noted, moreover, that as the repetition rate increases, the local velocity maximum occurs nearer the wall, indicating that the vibrational Reynolds number is effectively higher than the basic value for the case.

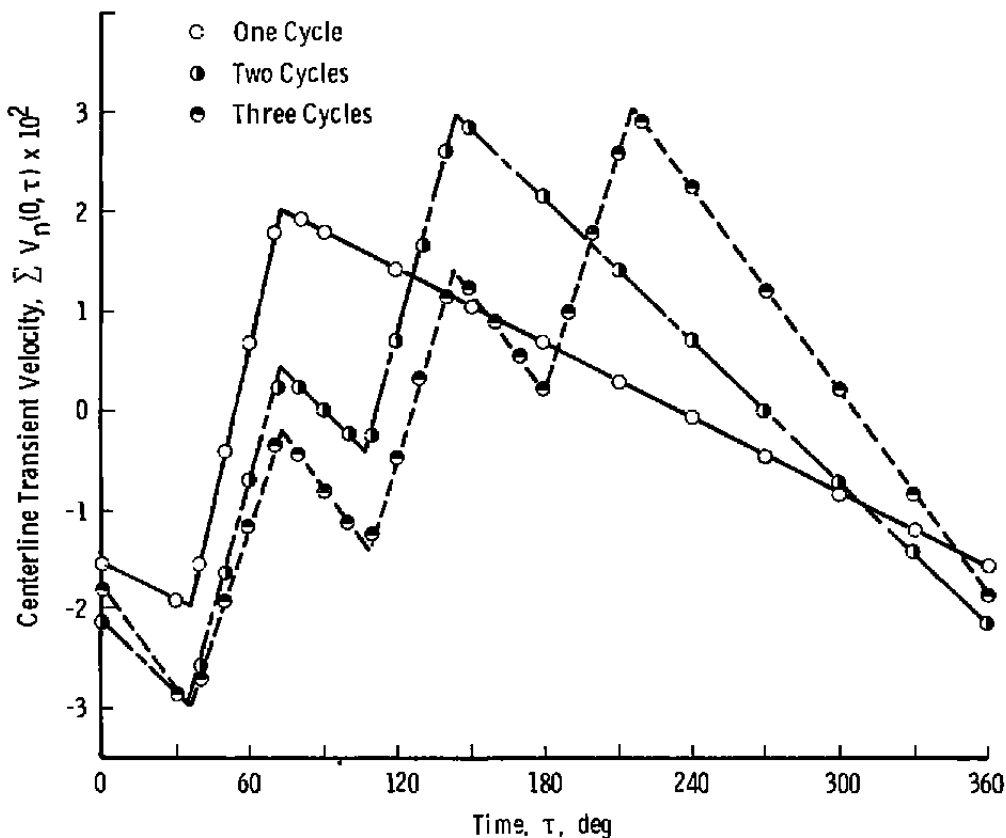


Figure 22. Centerline velocity response to asymmetric waves.

5.0 CONCLUSIONS AND RECOMMENDATIONS

An analysis was performed and computer programs were written to allow assessment of the velocity field in the fully developed region of a pipe for laminar or turbulent, steady or pulsating flows. For pulsating flows no restriction on waveform or the origin of the disturbance is imposed except that it be applied longitudinally.

For any waveform investigated, it was shown that, in the core of the pipe, the fluid velocity at any time during a cycle is an integral transform of the imposed pulsation. Near the tube wall, viscous effects become important, and the velocity may exceed that observed on the centerline. The extent of this annular flow region is dictated solely by the vibrational Reynolds number, the effect being confined nearer the tube wall as Re_v increases. The value of the maximum velocity relative to the core value varies in a complex fashion, initially increasing with frequency but decreasing for high frequencies. The overall level of the transient velocity, however, varies directly with a generalized amplitude and decreases with

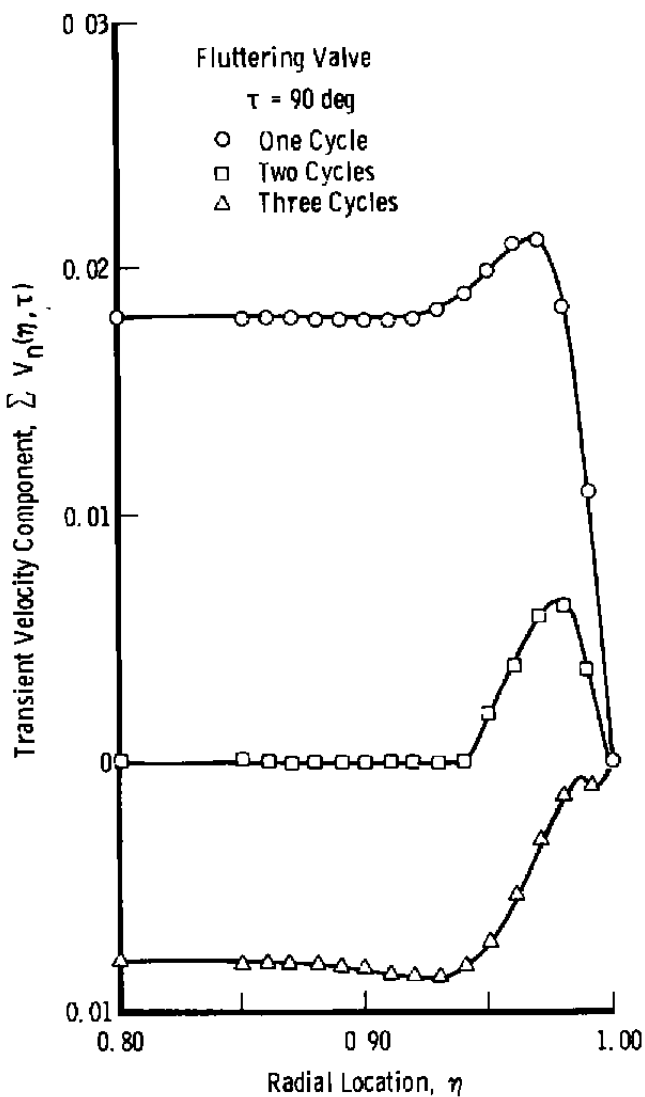


Figure 23. Distribution of transient velocity with radial location.

vibrational Reynolds number. Limited comparisons of the analysis with published data obtained for a vibrating tube show good agreement for no mean flow and laminar mean flow cases. In turbulent mean flows, however, the analysis agreed with the data at some times during a cycle but overpredicted the effect of pulsations at others. A crude estimate of the effect of alteration of the turbulent exchange mechanisms was found unsatisfactory for explaining the discrepancy.

A limited study of the effect of waveform on fluid response showed that the above general observations were valid for any waveform. For symmetrical waves it was found that

the magnitude and radial or temporal variations in velocity were, in a practical sense, virtually independent of waveform. Asymmetric waves, however, were shown to exhibit significantly different behavior.

The computer programs developed for the study were found to be satisfactory although several improvements are warranted. First, a test of the convergence of the Fourier series and velocity series would be of benefit in reducing the arbitrary waveform execution time. Secondly, several features of the harmonic oscillation code, such as strength of pulsation, rms velocity, and a vibrational Reynolds number calculation, should be included in the arbitrary waveform code. Finally, both programs should be extended to provide computer plotting of the results. It should be noted, moreover, that the steady flow routine incorporated in either program affords a simple, fast, and accurate method for computing the velocity distribution in fully developed laminar and turbulent flows.

The present study has clearly shown that the complexity of time-dependent flows for even a relatively simple case precludes the extrapolation of steady flow results into the transient domain. It is recommended, therefore, that work be continued at AEDC on transient flow phenomena. Two (ideally, parallel) approaches are suggested: (1) the present "exact" analysis should be extended to (a) treat the developing pulsating flow in a tube and (b) account for turbulent exchange mechanisms by the method of Appendix A; (2) time-dependent numerical solutions of the governing equations should be developed since they offer the only practical long range, general solutions. In addition, consideration should be given to longer range projects which (1) treat compressibility phenomena in transient flows and (2) obtain basic data on the effect of flow oscillations of various waveforms on the velocity field, turbulent structure, and skin friction. The first study is of importance since compressibility effects can have a significant effect on the velocity field development because wave propagation characteristics can be altered and secondary flows induced. An experimental program is required, moreover, to serve as a guide for modeling the effect of pulsations on turbulent structure. In particular, little or no data exist on the effect of waveform on the turbulent structure in pulsating flows.

Finally, it has been shown that flow pulsations can have a profound effect on heat transfer. Although myriad experiments have been performed and analyses presented, no definitive conclusions can yet be offered on the effect of pulsations on heat transfer (Refs. 4 and 8). An understanding of the mechanisms involved could possibly lead to revisions in the design of heat exchange devices.

REFERENCES

1. Richardson, E. G. and Tyler, E. "The Transverse Velocity Gradient Near the Mouths of Pipes in Which an Alternating or Continuous Flow of Air is Established." *The Proceedings of the Physical Society*, Vol. 42, Part I, No. 231, Dec. 16, 1929, pp. 1-15.
2. Uchida, S. "The Pulsating Viscous Flow Superimposed on the Steady Laminar Motion of Incompressible Fluid in a Circular Pipe." *ZAMP*, Vol. 7, Part 5, 1956, pp. 404-422.
3. Romie, F. E. "Heat Transfer to Fluids Flowing with Velocity Pulsations in a Pipe." Ph.D. Dissertation, UCLA, 1956.
4. Barnett, D. O. "An Analytical Investigation of Heat Transfer in Pulsating Turbulent Flow in a Tube." Ph.D. Dissertation, Auburn University, 1970.
5. Feiler, C. E. "Experimental Heat-Transfer and Boundary-Layer Behavior with 100-CPS Flow Oscillations. NASA TN D-2521, December 1964.
6. Bogdonoff, D. W. "A Study of the Mechanisms of Heat Transfer in Oscillating Flow." TR 483-f, Department of Aerospace and Mechanical Sciences, Princeton University, 1967.
7. Clamen, M. and Minton, P. "An Experimental Investigation of Flow in an Oscillating Pipe." *Journal of Fluid Mechanics*, Vol. 81, Part 3, July 13, 1977.
8. Richardson, P. D. "Effects of Sound and Vibrations on Heat Transfer." *Applied Mechanics Reviews*, Vol. 20, No. 3, March 1967.
9. Sexl, T. "'Annular Effect' in Resonators Observed by E. G. Richardson." *Zeitschrift für Physik*, Vol. 61, 1930, pp. 349-362.
10. Atabek, H. B. and Chang, C. C. "Oscillatory Flow Near the Entrance of a Circular Tube." *ZAMP*, Vol. 12, 1961, pp. 185-201.
11. Rouse, H. (Ed). *Advanced Mechanics of Fluids*. John Wiley and Sons, Inc., New York, 1963.
12. Parker, J. D., Boggs, J. H., and Blick, E. F. *Introduction to Fluid Mechanics and Heat Transfer*. Addison Wesley Publishing Co., Reading, Massachusetts, 1974.

13. Pai, S. I. "On Turbulent Flow in a Circular Tube." *J. Franklin Institute*, Vol. 256, No. 4, October 1953, pp. 337-352.
14. Haberstroh, R. D. and Baldwin, L. V. "Application of a Simplified Velocity Profile to the Prediction of Pipe-Flow Heat Transfer." *Transactions of the ASME, in Journal of Heat Transfer*, Vol. 90, No. 4, 1968, p. 191.
15. Mickelsen, W. R. and Laurence, J. C. "Measurement and Analysis of Turbulent Flow Containing Periodic Flow Fluctuations." *NACA RM E53F19*, August 1953.
16. McLachlan, N. W. *Bessel Functions for Engineers*. Clarendon Press, Oxford, 1955 (Second Edition).
17. Jenkins, G. M. and Watts, D. G. *Spectral Analysis and Its Applications*. Holden-Day, San Francisco, 1969.
18. Madzumder, M. K. and Kirsch, K. J. "Aerosol Size Spectrum by Laser Doppler Velocimeter." *Minnesota Symposium on Laser Anemometry*, University of Minnesota, October 1975.
19. Richardson, E. G. *Dynamics of Real Fluids*. Arnold Ltd., London, 1961.
20. Richardson, E. G. "The Amplitude of Sound Waves in Resonators." *Proceedings of the Physical Society*, Vol. 40, No. 206, 1928.
21. Mohajery, M. "An Experimental Study of the Structure of the Pulsating Turbulent Flow of Air in a Circular Pipe." Ph.D. Dissertation, Clarkson College of Technology, 1973.
22. Carnahan, B., Luther, H. A., and Wilkes, J. O. *Applied Numerical Methods*. John Wiley and Sons, Inc., New York, 1969.
23. Wolfe, P. "The Secant Method for Simultaneous Non-Linear Equations." *ACM Communications*, Vol. 2, No. 12, 1959.
24. Johnson, D. E. and Johnson, J. R. *Mathematical Methods in Engineering and Physics*. Ronald Press, New York, 1965.

APPENDIX A

FORMULATION FOR ARBITRARY EDDY VISCOSITY MODEL

The radial distribution function for the transient velocity component, $f(\eta)$, is given by an equation of the form

$$af'' + \beta f' - i\gamma f = -Q \quad (A-1)$$

where primes denote differentiation with respect to η and

$$\alpha(\eta) = 1 + \frac{\epsilon_m}{\nu} \quad (A-2)$$

$$\beta(\eta) = \frac{1}{\eta} \alpha(\eta) + \frac{\epsilon_m'}{\nu} \quad (A-3)$$

$$\gamma = Re_v \quad (A-4)$$

In general, $f(\eta)$ is a complex function and may be written

$$f(\eta) = f_r(\eta) + i f_i(\eta) \quad (A-5)$$

where $f_r(\eta)$ and $f_i(\eta)$ are the real and imaginary parts, respectively, of the function.

Substituting Eq. (A-5) into Eq. (A-1) and requiring a , α , β , and γ to be real functions leads to the following simultaneous equations:

$$-a = af_r'' + \beta f_r' + \gamma f_i' \quad (A-6)$$

$$f_r = \frac{a}{\gamma} f_r'' + \frac{\beta}{\gamma} f_i' \quad (A-7)$$

The real part of the distribution is thus determined once f_i and its derivatives are known.

Differentiating Eq. (A-7) and substituting in Eq. (A-6) leads to the following fourth-order differential equation:

$$A(\eta) f_i^{(IV)} + B(\eta) f_i^{(III)} + C(\eta) f_i^{(II)} + D(\eta) f_i^{(I)} + E f_i = -F \quad (A-8)$$

where

$$\left. \begin{aligned}
 A(\eta) &= \alpha^2 \\
 B(\eta) &= 2\alpha(\alpha' + \beta) \\
 C(\eta) &= \alpha(\alpha'' + 2\beta') + \beta(\alpha' + \beta) \\
 D(\eta) &= \alpha\beta'' + \beta\beta' \\
 E &= \gamma^2 \\
 F &= Q_\gamma
 \end{aligned} \right\} \quad (A-9)$$

Thus, if ϵ_{m_1} can be described by any analytic function with continuous second derivatives, the coefficients are uniquely determined. Equation (A-8), moreover, may be solved by any of several numerical methods for ordinary differential equations (Ref. 22). The solution, however, will require initial estimates of f_i and its derivatives at one or more points in the flow and satisfaction of the boundary condition $f_i(1) = 0$. These estimates may readily be obtained from the $\epsilon_{m_1} = \text{constant}$ solution of Eq. (80).

One solution procedure which has been programmed in Fortran IV involves reducing the order of Eq. (A-8) by introducing the relations

with

$$\left. \begin{aligned}
 g_n &= g'_{n-1} & (n > 1) \\
 g_1 &= f'_i
 \end{aligned} \right\} \quad (A-10)$$

Equation (A-8) is thus reduced to a series of first-order simultaneous equations:

$$g'_3 = -\frac{1}{\Lambda} \left[Bg_3 + Cg_2 + Dg_1 + Ef_i + F \right] \quad (A-11)$$

$$\left. \begin{aligned} g_2' &= g_3 \\ g_1' &= g_2 \\ f_1' &= g_1 \end{aligned} \right\} \quad \begin{aligned} & \text{(A-11)} \\ & \text{Concl.} \end{aligned}$$

Integration of each equation was accomplished using a fourth-order Runge-Kutta method in conjunction with the secant method for simultaneous nonlinear equations (Ref. 23). The real part of the distribution function is then

$$f_r = \frac{\alpha}{\gamma} g_2 + \frac{\beta}{\gamma} g_1 \quad \text{(A-12)}$$

The transient velocity at each point of the flow field is

$$V_1(\eta, \tau) = f_r(\eta) \cos \tau - f_1(\eta) \sin \tau \quad \text{(A-13)}$$

and the instantaneous velocity profile is

$$V(\eta, \tau) = V_o(\eta) + V_1(\eta, \tau) \quad \text{(A-14)}$$

with $V_o(\eta)$ given by Eq. (46).

APPENDIX B

A NOTE ON COMPLEX FOURIER EXPANSIONS

The Fourier trigonometric expansion of an arbitrary periodic function, $f(t)$, which satisfies the Dirichlet conditions (Ref. 24) may be written

$$f(t) = \frac{A_0}{2} + \sum_{n=1}^{\infty} A_n \cos n\omega t + \sum_{n=1}^{\infty} B_n \sin n\omega t \quad (B-1)$$

where the Fourier coefficients are given by the transforms

$$A_n = \frac{2}{P} \int_{C}^{C+P} f(t') \cos (n\omega t') dt'; n = 0, 1, 2, \dots \quad (B-2)$$

and

$$B_n = \frac{2}{P} \int_{C}^{C+P} f(t') \sin (n\omega t') dt'; n = 1, 2, \dots \quad (B-3)$$

The basic period of the function is $P = 2\pi/\omega$, and $n\omega$ represent the various harmonics of Ω .

It is often convenient to express Eq. (B-1) in its equivalent complex form,

$$f(t) = \sum_{n=-\infty}^{\infty} K_n e^{in\omega t} \quad (B-4)$$

which is readily obtained by a direct substitution of the complex definitions of the sine and cosine into the trigonometric series. When that is done, the coefficients are defined by

$$K_n = \frac{1}{P} \int_{P}^{C+P} f(t') e^{-in\omega t'} dt' \quad (B-5)$$

or

$$K_n = \frac{1}{2} \left\{ A_n - i B_n \right\} \quad (B-6)$$

The functions $f(t)$ considered in this report are always real; thus it is possible to rewrite Eq. (B-4) in a form that is more amenable to computation. For this purpose, the complex expansion is rewritten as

$$f(t) = H_0 + \sum_{n=1}^{\infty} H_n e^{in\omega t} + \sum_{|n|=1}^{\infty} H_{-|n|} e^{-i|n|\omega t} \quad (B-7)$$

where H_n is still given by Eq. (B-5) or (B-6) but

$$H_{-|n|} = \frac{1}{P} \int_C^{C+P} f(t') e^{i|n|\omega t'} dt' \quad (B-8)$$

and

$$H_{-|n|} = \frac{1}{2} \left\{ A_n - i B_n \right\} \quad (B-9)$$

Comparing Eqs. (B-6) and (B-9), one sees that H_n and $H_{-|n|}$ are complex conjugates. The terms to be summed in Eq. (B-7) are, likewise, complex conjugates. Thus, for any real function $f(t)$, Eq. (B-7) becomes

$$f(t) = H_0 + 2 \sum_{n=1}^{\infty} H_n e^{in\omega t} \quad (B-10)$$

where it is understood that n is a positive integer and the coefficients are defined by Eq. (B-6).

NOMENCLATURE

A	Dimensionless vibration amplitude, Z_0/R
A_n	Fourier Cosine Transform, Eq. (71)
A_p	Dimensionless pressure amplitude, Ω_1/Ω_0
a*	Frequency parameter, $(Re_s)^{1/2}$
g	Generalized amplitude, Eq. (40)
g*	Modified amplitude, Eq. (54)
B_a	Fourier Sine Transform, Eq. (72)
b	Mean value of arbitrary parameter
C	Constant
C_f	Fanning friction factor, $\phi_w/\rho \hat{U}^2$
F₀(η,t)	Arbitrary function, Eq. (28)
F(t)	Arbitrary forcing function, Eq. (40)
f(η)	Radial distribution function, Eq. (57)
f_i(η)	Imaginary part of distribution function, Eq. (80)
f_r(η)	Real part of distribution function, Eq. (79)
G*	Dimensionless mass flow rate, Eq. (33)
H_n	Complex Fourier Coefficient, Eq. (62)
I_ν(i^{1/2}x)	Modified Bessel function of first kind
K_ν(i^{1/2}x)	Modified Bessel function of second kind
M_ν(x)	Modulus of polar representation of $I_{\nu}(i^{1/2}x)$
m	Empirical coefficient, Eq. (49)
ṁ	Mass flow rate (M/t)

n	nth harmonic or term
P	Instantaneous pressure (m/Lt^2) or period (t)
p	Mean pressure (M/Lt^2)
p'	Fluctuating pressure (M/Lt^2)
p^*	Reference pressure (M/Lt^2)
R	Tube radius (L)
Re	Mean throughflow Reynolds number, $2\langle \bar{U} \rangle R/\nu$
Re^*	Friction Reynolds number, U^*R/ν
Re_n	Harmonic Reynolds number, $\omega Z_o R/\nu$
Re_v	Vibrational Reynolds number, $\omega R^2/\nu$
Re_v^*	Modified vibrational Reynolds number, $Re_v \sqrt{1 + (\epsilon_m/\nu)}$
R_{uiuj}	Correlation coefficient, $\overline{u_i' u_j'}/U^{*2}$
(r, θ, z)	Noninertial cylindrical coordinate system
(r', θ', z')	Inertial cylindrical coordinate system
S	Pulsation strength, Eq. (82)
s	Empirical coefficient, Eq. (48)
T	Time interval (t)
t	Time (t)
$(\bar{U}, \bar{V}, \bar{W})$	Reference frame velocity (L/t)
U_h	Harmonic velocity, $\omega Z_o (L/t)$
U^*	Friction velocity, $\sqrt{\langle \sigma_w \rangle / \rho}$
(u, v, w)	Mean velocity components (L/t)
(u', v', w')	Fluctuating velocity components (L/t)

V_1	Dimensionless transient velocity
V_c	Centerline velocity, $W(0,t)/U^*$
V_i	Instantaneous velocity, $w(r,t)/U^*$
\tilde{V}_i	Reference frame velocity component (L/t)
V_o	Dimensionless mean velocity
v_i	Mean velocity component (L/t)
v'_i	Fluctuating velocity component (L/t)
$\overline{v'_i v'_j}$	Reynolds stress component
X_i	Body force (ML/t^2)
x_i, x_j	Cartesian coordinates
\bar{x}	Time mean value, $1/T \int_0^T x dt$
$\langle x \rangle$	Mean value over a cycle, $1/2\pi \int_0^{2\pi} x dt$
\hat{x}	Spatial mean value, $\int_0^1 x \eta d\eta$
Z_o	Vibration amplitude (L)
Δ	Cubical dilation,
δ	Boundary-layer thickness (L)
ϵ_{m0}	Eddy viscosity of mean flow (L^2/t)
ϵ_{m1}	Eddy viscosity of transient flow (L^2/t)
ξ	Dimensionless axial coordinate, Z/R
η	Dimensionless radial coordinate, r/R
Λ_n	Fourier coefficient relations, Eqs. (74) and (75)
μ	Absolute viscosity, (M/Lt)
μ_o	Bulk viscosity, (M/Lt)

ν	Kinematic viscosity (L^2/t) or order of Bessel function
$\theta_\nu(x)$	Phase of polar representation of $I_\nu (i^{1/2}x)$
ρ	Density (M/L^3)
σ_w	Wall shear stress, (M/Lt^2)
τ	Dimensionless time, ωt
Ω	Pressure coefficient, $P - P^*/\rho U^*{}^2$
Ω_0	Mean flow pressure coefficient
Ω_1	Transient component of pressure coefficient
ω	Frequency ($1/t$)